

CHAPTER 2

BACKGROUND AND LITERATURE REVIEW

This chapter describes the background of piezoelectricity, ferroelectrics, polyvinylidene fluoride (PVDF), portland cement (PC), carbon graphite (C) and composite. The review of literatures related to cement based piezoelectric composite, microstructure and electrical properties of composites investigated in this project are given. Moreover, cement based piezoelectric composite with third phase addition from literatures are also given.

2.1 Piezoelectric ceramics

2.1.1 Background and basis for piezoelectricity Theory

All materials undergo a small change in dimensions when subjected to an electric field. If the resultant strain is proportional to the square of the field it is known as the electrostrictive effect. Some materials show the reverse effect – the development of electric polarization when they are strained through an applied stress. These are said to be piezoelectric (pronounced ‘pie-ease-oh’). To a first approximation the polarization is proportional to the stress and the effect is said to be ‘direct’. Piezoelectric materials also show a ‘converse’ effect, i.e. the development of a strain x directly proportional to an applied field [18-21].

Piezoelectricity, a property possessed by a select group of materials, was discovered in 1880 by Jacques and Pierre Curie during their systematic study of the effect of pressure on the generation of electrical charge by crystals, such as quartz,

zincblende, and tourmaline. The name “piezo” is derived from the Greek, meaning “to press;” hence, piezoelectricity is the generation of electricity as a result of a mechanical pressure. Cady [22] defines piezoelectricity as “electric polarization produced by mechanical strain in crystals belonging to certain classes, the polarization being proportional to the strain and changing sign with it.”

To understand a phenomenon of piezoelectricity, one must consider atomic structure level of materials and principal distribution of ions within individual crystallites. The arrangements of ions are constrained to minimum energy positions, resulting in repeating spatial relationships that define unit cell of crystal lattice. All crystals may be divided into 32 crystallographic classes depending on geometry and symmetry of unit cell. Twenty one of these classes are noncentrosymmetric, of which all but one (due to other symmetry elements) exhibit piezoelectricity [10]. For a strained crystal without central symmetry, movements of positive and negative ions with respect to one another will produce a net polarization and associated electric dipole. Conversely, application of an electric field across unit cell will cause ionic movement, since alignment with a direction of a field is preferable, producing a charge in dimension of a crystal and strain in a material at a macroscopic level.

2.1.2 Piezoelectricity in ferroelectric ceramics

As mentioned previously, the poling process is the critical element in being able to utilize the piezoelectric effect in a ferroelectric ceramic. Without poling, the ceramic is inactive, even though each one of the individual crystallites is piezoelectric itself [10]. With poling, however, the ceramic becomes extremely useful, provided that it is not heated above its Curie temperature (T_C), where it loses its polarization

and all of the orientation of the polarization produced by the poling process [23]. Two effects are operative in piezoelectric crystals, in general, and in ferroelectric ceramics, in particular. The direct effect (designated as a generator) is identified with the phenomenon whereby electrical charge (polarization) is generated from a mechanical stress, whereas the converse effect (designated as a motor) is associated with the mechanical movement generated by the application of an electrical field. Both of these effects are illustrated in Fig. 1 as cartoons for easy grasp of the principles. The basic equations that describe these two effects in regard to electric and elastic properties are [1, 18].

$$D = dE + \varepsilon^T E \quad (\text{generator}) \quad (2.1)$$

$$S = s^E T + dE \quad (\text{motor}) \quad (2.2)$$

where D is the dielectric displacement (consider it equal to polarization), T the stress, E the electric field, S the strain, d a piezoelectric coefficient, s the material compliance (inverse of modulus of elasticity), and ε the dielectric constant (permittivity). The superscripts indicate a quantity held constant: in the case of ε^T , the stress is held constant, which means that the piezoelectric element is mechanically unconstrained, and, in the case of s^E , the electric field is held constant, which means the electrodes on the element are shorted together. Equations (1) and (2), in matrix form, actually describe a set of equations that relate these properties along different orientations of the material. Because of the detailed nature of the many equations involved [18, 24, 25].

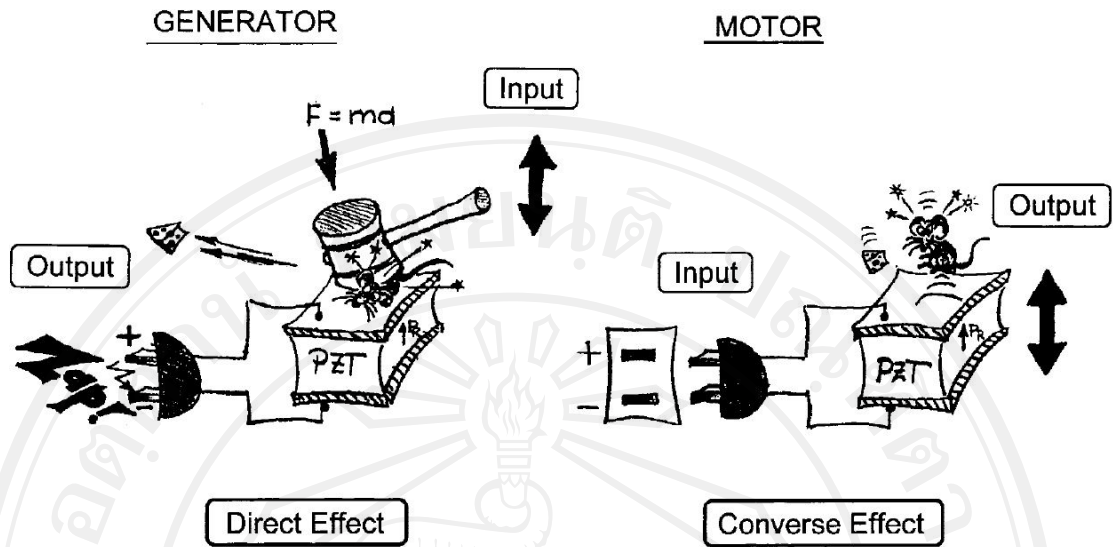


Fig 2.1 Piezoelectric effects in ferroelectric ceramics [10]

Suffice it to say that, because this is a piezoelectric solid, Equations. (1) and (2) relate given properties, such as electric displacement (polarization) and strain to both the mechanical and electrical states of the material. Furthermore, these properties are directional quantities, and, hence, they are usually specified with subscripts to identify the conditions under which they are determined, e.g., d_{31} indicates that this piezoelectric coefficient relates to the generation of polarization (direct effect) in the electrodes perpendicular to the 3 or vertical direction and to the stress mechanically applied in the 1 or lateral direction; d_{33} indicates the polarization generated in the 3 direction when the stress is applied in the 3 direction. Typical relationships for this coefficient are:

$$D_3 = d_{33}T_3 \text{ (direct effect)} \quad (2.3)$$

$$S_3 = d_{33}E_3 \text{ (converse effect)} \quad (2.4)$$

where the d coefficients are numerically equal in both equations. The d coefficients are usually expressed as $\times 10^{-12}$ C/N for the direct effect and $\times 10^{-12}$ m/V for the

converse effect. High d coefficients are desirable for those materials that are utilized in motional or vibrational devices, such as sonar and sounders. In addition to the d coefficients, open-circuit g coefficients are also used to evaluate piezoelectric ceramics for their ability to generate large amounts of voltage per unit of input stress. The g constant is related to the d constant via the relationship

$$g = d / \epsilon_r \epsilon_0 \quad (2.5)$$

where ϵ_r is the relative dielectric constant and ϵ_0 the permittivity of free space (8.854×10^{-12} F/m). Thus, a high g constant is possible for a given d coefficient if the material has a low ϵ_r . High- g -constant ceramics are usually ferroelectrically hard materials that do not switch their polarization readily and possess lower ϵ_r values. They are used in devices such as portable gas ignitors and patio lighters. The piezoelectric coupling factor is a convenient and direct measurement of the overall strength of the electromechanical effect, i.e., the ability of the ceramic transducer to convert one form of energy to another. It is defined as the square root of the ratio of energy output in electrical form to the total mechanical energy input (direct effect), or the square root of the ratio of the energy available in mechanical form to the total electrical energy input (converse effect). Because the conversion of electrical to mechanical energy (or vice versa) is always incomplete.

All of the properties mentioned here may be realized in a piezoelectric ceramic, which is, in reality, a poled ferroelectric ceramic material. During the process of poling, there is a small expansion of the material along the poling axis and a slight contraction in both directions perpendicular to it. The strength of the poling field, often in combination with elevated temperature, is an important factor in determining the extent of alignment and, hence, the resulting properties. Alignment is never

complete; however, depending on the type of crystal structure involved, the thoroughness of poling can be quite high, ranging from 83% for the tetragonal phase to 86% for the rhombohedral phase, and to 91% for the orthorhombic phase, when compared with single-domain, single-crystal values. Because all ceramic bodies are macroscopically isotropic in the “as-sintered” condition and must be poled to render them useful as piezoelectric materials, they are all ferroelectric as well as piezoelectric.

2.1.3 Hysteresis loops

The hysteresis loop (polarization versus electric field) is the single most important measurement that can be made on a ferroelectric ceramic when characterizing its electrical behavior [10]. This loop is very similar to the magnetic loop (magnetization versus magnetic field) one obtains from a ferromagnetic material; the very name “ferroelectric” has been appropriated from this similarity, even though there is no ferro, i.e., iron constituent, in ferroelectrics as a major component [10].

Hysteresis loops come in all sizes and shapes, and, similar to a fingerprint, identify the material in a very special way. Therefore, one should become familiar with such a measurement. Although early workers in the field of ferroelectrics utilized a dynamic (60 Hz) measurement with a Sawyer–Tower circuit and an oscilloscope readout, more-recent work usually has been done with a single-pulse or dc (~0.1 Hz) Sawyer–Tower measurement using an X–Y plotter or computer readout [26].

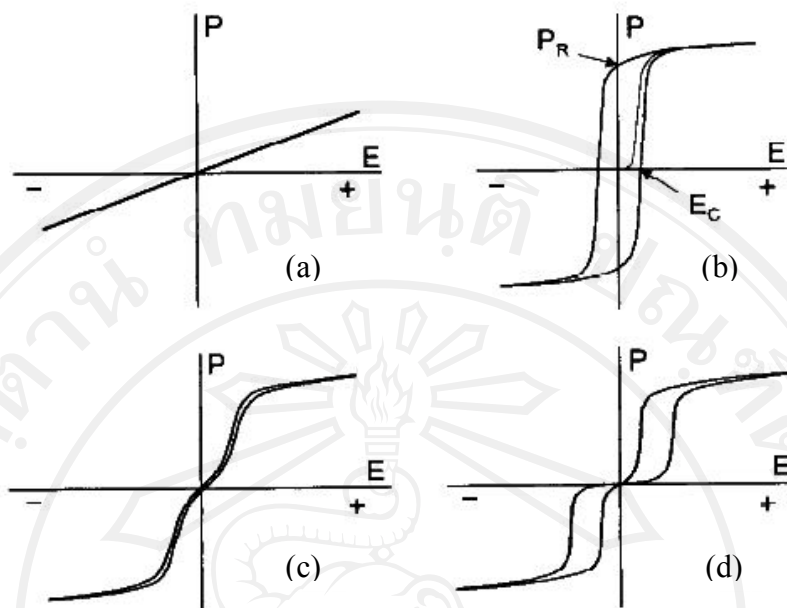


Fig 2.2 Typical hysteresis loops from various ferroelectric ceramics: (a) BaTiO₃ capacitor, (b) soft (easily switchable) PZT, (c) PLZT relaxor, and (d) PSZT antiferroelectric material [10]

Typical hysteresis loops obtained from various ferroelectric ceramic materials are illustrated in Fig. 2.2: (a) a linear tracing from a BaTiO₃ capacitor, (b) a highly nonlinear loop from a low-coercive-field (soft) memory ferroelectric such as is found in the rhombohedral region of the PZT phase diagram, (c) a narrow, nonlinear loop obtained from a slim-loop ferroelectric (SFE) quadratic relaxor that is located in the FE–PE boundary region of the PLZT system, and (d) a double loop that typically is obtained from a nonmemory antiferroelectric material in the PSZT system.

The antiferroelectric materials are essentially nonpolar, nonferroelectric ceramics that revert to a ferroelectric state when subjected to a sufficiently high electric field. Outwardly, they differ from the SFE relaxor materials in that (1) the

dielectric constants usually are lower, (2) higher electric fields are usually required to induce the ferroelectric state, and (3) the onset of the ferroelectric state and the return of the antiferroelectric state are usually fairly abrupt, thus giving the loop an appearance of two subloops that are positively and negatively biased. These characteristics are shown in loop (d) in Fig. 2.2.

A considerable amount of information can be obtained from a hysteresis loop. Fig. 2.2 also shows that (1) the loop in (b) reveals that the material has memory, whereas the loop in (c) indicates no memory, (2) high remanent polarization (P_r) relates to high internal polarizability, strain, electromechanical coupling, and electrooptic activity, (3) for a given material, the switching field (E_c) is an indication of the grain size for a given material (i.e., lower E_c means larger grain size and higher E_c means smaller grain size), (4) a high degree of loop squareness usually indicates better homogeneity and uniformity of grain size, (5) an off-centered loop from the zero voltage point (the loop is usually centered symmetrically around zero voltage) indicates some degree of internal electrical bias that may be caused by internal space charge and/or aging, (6) the sharpness of the loop tips indicates a high electrical resistivity ($>10^9 \Omega \cdot \text{cm}$), (7) high induced polarization in relaxor materials indicates high electrostriction strain and high electrooptic coefficients, (8) the slope of the P - E loop at any point along the loop is equal to the large-signal dielectric constant, (9) the opening up of the loop of a SFE relaxor material can indicate nonohmic contact between the electrodes and the ceramic, and (10) a sudden large change in “apparent” polarization is usually a result of incipient dielectric breakdown. Remanent polarizations for most of the lead-containing ferroelectrics typically vary from 30 to 40 $\mu\text{C}/\text{cm}^2$, whereas the coercive fields vary over quite a wide range, from $\sim 2 \text{ kV}/\text{cm}$

to near electrical breakdown (~ 125 kV/cm), depending on the type of dopants and modifiers added.

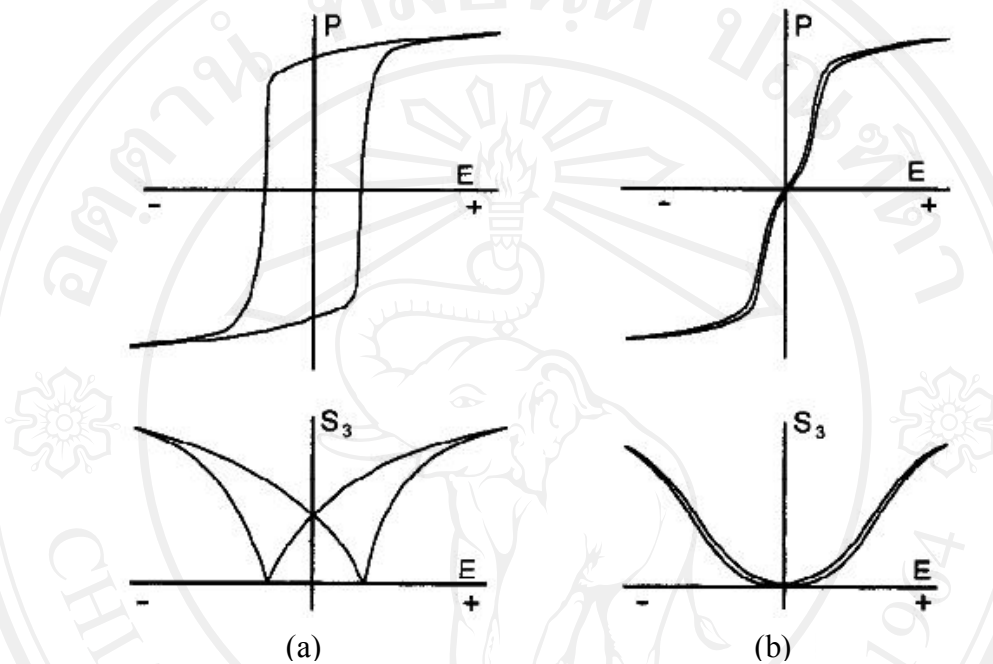


Fig 2.3 Hysteresis loops and longitudinal strain curves for (a) ferroelectric memory ceramic and (b) SFE nonmemory relaxor ceramic [10]

The strains associated with two of these materials (i.e., ferroelectric and SFE) on traversing their hysteresis loops are given in Fig. 2.3. In the ferroelectric case, the switching strain accompanying the polarization reversal process results in the familiar “butterfly” loop, with the remnant strain state in the center of the loop. Positive voltage then results in a longitudinal expansion of the ceramic, whereas a negative voltage (less than the coercive field) results in a longitudinal contraction.

This is known as the linear strain effect in piezoelectric materials and does not involve domain switching. For the SFE relaxor case, there is no remnant strain when

the electric field is not applied, because, in this case, the rest position of the ion is in the center of the unit cell. However, when the field is applied, ionic movement (polarization) and strain occur simultaneously, both being dependent upon the strength of the field. Because the sign of the strain produced (positive for elongation) is the same regardless of the polarity of the field, this is the electrostrictive effect mentioned previously.

2.1.4 Poling

Before poling, ferroelectric ceramics do not possess any piezoelectric properties owing to the random orientations of the ferroelectric domains in the ceramics. During poling, a d.c. electric field is applied on the ferroelectric ceramic sample to force the domain to reorient. After poling, the electric field is removed and a remnant polarization and a remnant strain are maintained in the sample, and now the sample exhibits piezoelectricity. A simple illustration of the poling process is shown in Fig. 2.4.

During the poling process, it is important that appropriate poling field strength, temperature and time be chosen. Theoretically, when an external poling field is larger than the coercive field of a ferroelectric sample, most of the domain should be reoriented. However, it has been shown by experiments that a practical poling field must be 3 or 4 times the coercive field (that corresponds to the saturated portion of the hysteresis loop) before maximum piezoelectricity is obtained. It must be pointed out that both the coercive field and the saturation field decrease as the temperature increases. This is due to higher mobility of ferroelectric domains in the sample at higher temperatures.

When choosing a practical value of the poling field, the breakdown strength of the sample must be considered. In some cases, the breakdown of the sample occurs, even though the applied field is smaller than the saturation field. The breakdown strength depends on several factors: the ceramic composition, dopants, homogeneity, properties and crevices in the sample. The last three factors depend on the processing of the ceramics [28].

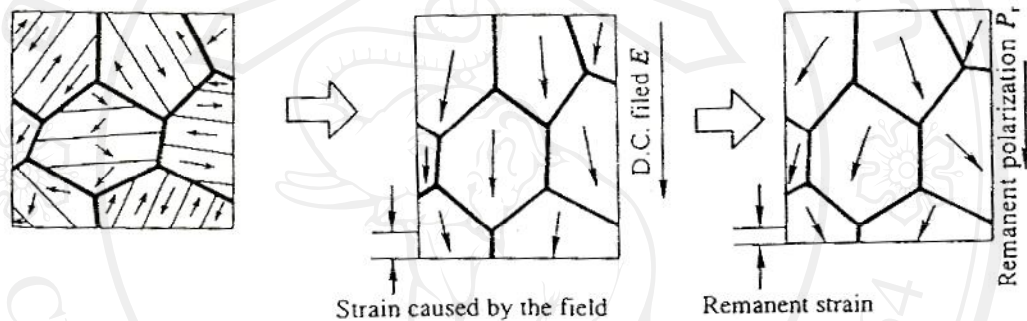


Fig 2.4 Schematic drawing of the poling process for piezoelectric ceramics [27]

For domain reorientation (or dipole rearrangement), a poling field must be applied on the sample and maintained for a certain length of time. For a given poling field and poling time, better domain rearrangement results at higher poling temperatures. This can be explained by the following arguments: Firstly, with increase poling temperature, crystalline anisotropy of ferroelectrics decreases. Secondly, when the temperature is higher, the hysteresis loop becomes narrower. Thus, as the temperature increases, the coercive field decreases, which allows easier domain movements. Thirdly, with increasing temperature, space charges, which act against domain motion, decrease in the ceramics.

In practice, one usually prefers higher rather than lower poling temperatures. However, when the poling temperature is too high, problems arise as the electrical conductivity increases, and the consequent increase in the leakage current would result in sample breakdown during the period of poling.

2.1.5 Lead zirconate titanate, PZT

The first piezoceramic to be developed commercially was BaTiO₃. By the 1950s the solid solution system Pb(Ti,Zr)O₃ (PZT), which also has the perovskite structure, was found to be ferroelectric and PZT compositions are now the most widely exploited of all piezoelectric ceramics [28].

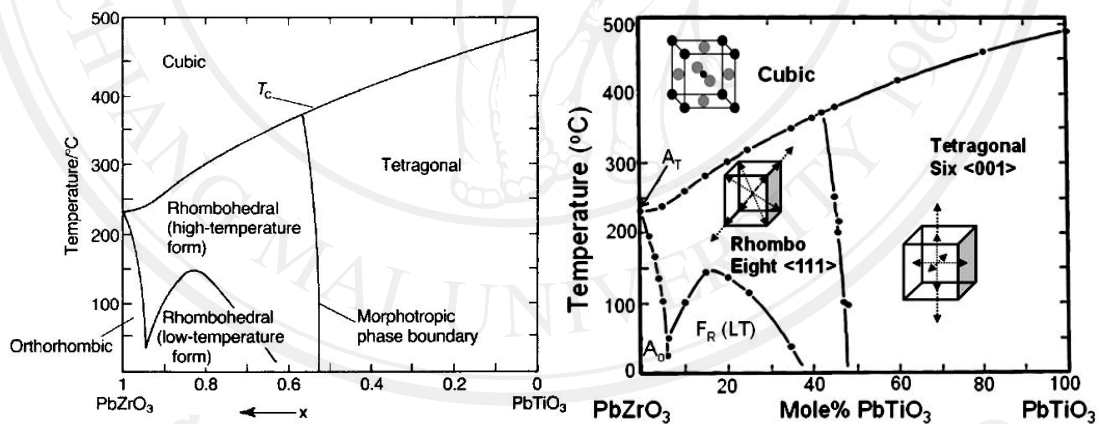


Fig 2.5 Morphotropic phase boundary in the Pb(Zr,Ti)O₃ system [18]

The Pb(Zr_{1-x}Ti_x)O₃ phase diagram [18] is shown in Fig. 2.5. The morphotropic phase boundary (MPB) defines the composition at which there is an abrupt structural change, the composition being almost independent of temperature. That is the phase boundary between the high temperature rhombohedral and tetragonal forms is, practically speaking, a vertical line. As shown in Fig. 2.6, the piezoelectric activity

peaks in the region of the MPB composition and considerable effort has been directed to elucidating the reason(s) for this technically very important phenomenon.

The current understanding is that the MPB is not a sharp boundary but rather a temperature-dependent compositional range over which there is a mixture of tetragonal and monoclinic phases. At room temperature (300 K) the two phases coexist over the range $0.455 \leq x \leq 0.48$ [29]. The enhanced piezoelectric activity of the commercial compositions ($x \sim 0.48$) can be rationalised in terms of the relatively large ionic displacements associated with stress (electrical or mechanical) – induced rotation of the monoclinic polar axis [30].

As a ferroelectric perovskite in ceramic form cools through its Curie point it contracts isotropically since the orientations of its component crystals are random. However, the individual crystals will have a tendency to assume the anisotropic shapes required by the orientation of their crystal axes. This tendency will be counteracted by the isotropic contraction of the cavities they occupy. As a consequence a complex system of differently oriented domains that minimizes the elastic strain energy within the crystals will become established.

The application of a sufficiently strong field will orient the 180° domains in the field direction, as nearly as the orientation of the crystal axes allows. The field will also have an orienting effect on 90° domains in tetragonal material and on 71° and 109° domains in the rhombohedral form, but the response will be limited by the strain situation within and between the crystals. There will be an overall change in the shape of the ceramic body with an expansion in the field direction and a contraction at right angles to it. When the field is removed the strain in some regions will cause the polar

orientation to revert to its previous direction, but a substantial part of the reorientation will be permanent.

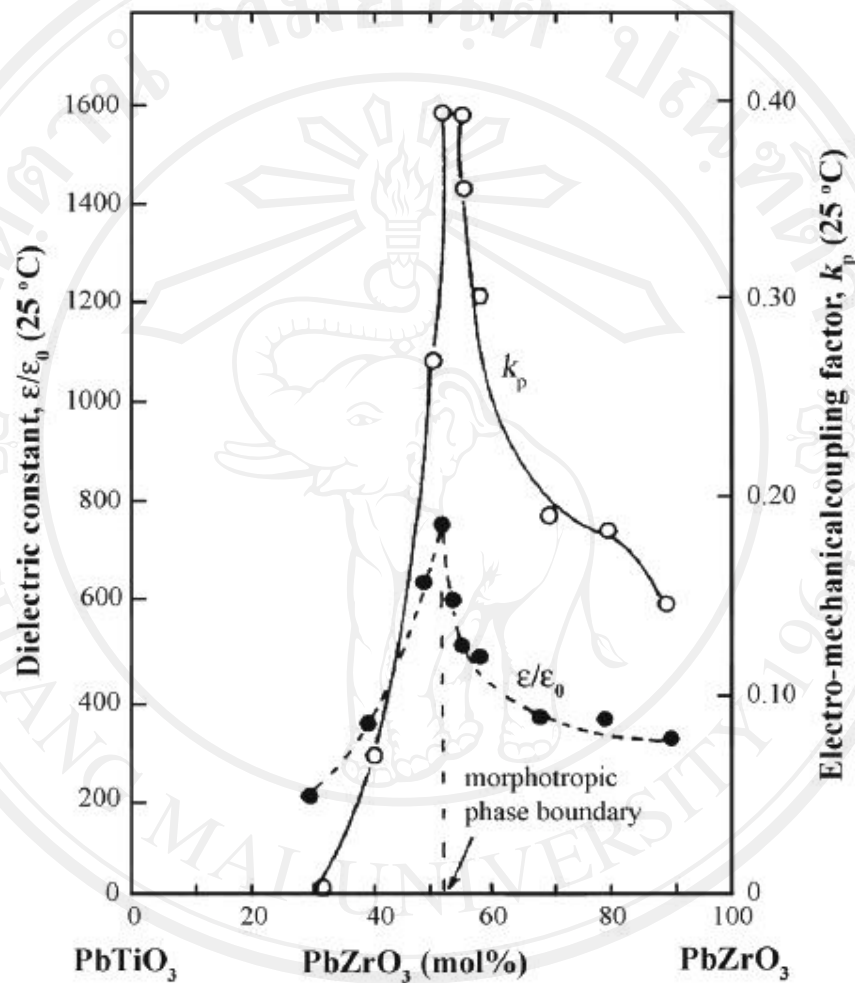


Fig 2.6 Composition dependence of dielectric constant and electromechanical coupling factor in PZT ceramic [27]

An externally applied stress will affect the internal strain and the domain structures will respond; this process is termed the ferroelastic effect. Compression will favour polar orientations perpendicular to the stress while tension will favour a parallel orientation. Thus the polarity conferred by a field through 90° domain

changes can be reversed by a compressive stress in the field direction. Stress will not affect 180° domains except in so far as their behaviour may be coupled with other domain changes. A polar axis can be conferred on the isotropic ceramic by applying a static field of $1\text{--}4 \text{ MVm}^{-1}$ for periods of several minutes at temperatures usually somewhat above 100°C when domain alignment occurs. More rapid domain movement takes place at higher temperatures but the maximum alignment of 90° domains takes some time to be established.

The temperature is limited by the leakage current which can lead to an increase in the internal temperature and to thermal breakdown; the field is limited by the breakdown strength. If the applied voltage exceeds about 1 kV it is necessary to ensure very clean surfaces between the electrodes and to immerse the pieces to be poled in insulating oil. Surface breakdown takes place very readily between electrodes on the surface of a high-permittivity material when it is exposed to air.

Depoling can be achieved by applying a field in the opposite direction to that used for poling or, in some cases, by applying a high a.c. field and gradually reducing it to zero, but there is a danger of overheating because of the high dielectric loss at high fields. Some compositions can be depoled by applying a compressive stress (10–100 MPa). Complete depoling is achieved by raising the temperature to well above the Curie point and cooling without a field.

Alternating fields cause domain walls to oscillate. At low fields the excursions of 90° , 71° or 109° walls result in stress–strain cycles that lead to the conversion of some electrical energy into heat and therefore contribute to the dielectric loss. When peak fields are sufficient to reverse the spontaneous polarization the loss becomes very high, as shown by a marked expansion of the hysteresis loop (Fig. 2.7). Fig 2.8

(a) and (b) show variations, at room temperature of piezoelectric coefficient d_{ij} [18] and remanent polarization P_r [31], respectively with composition in PZT piezoelectric ceramics near the morphotropic phase boundary.

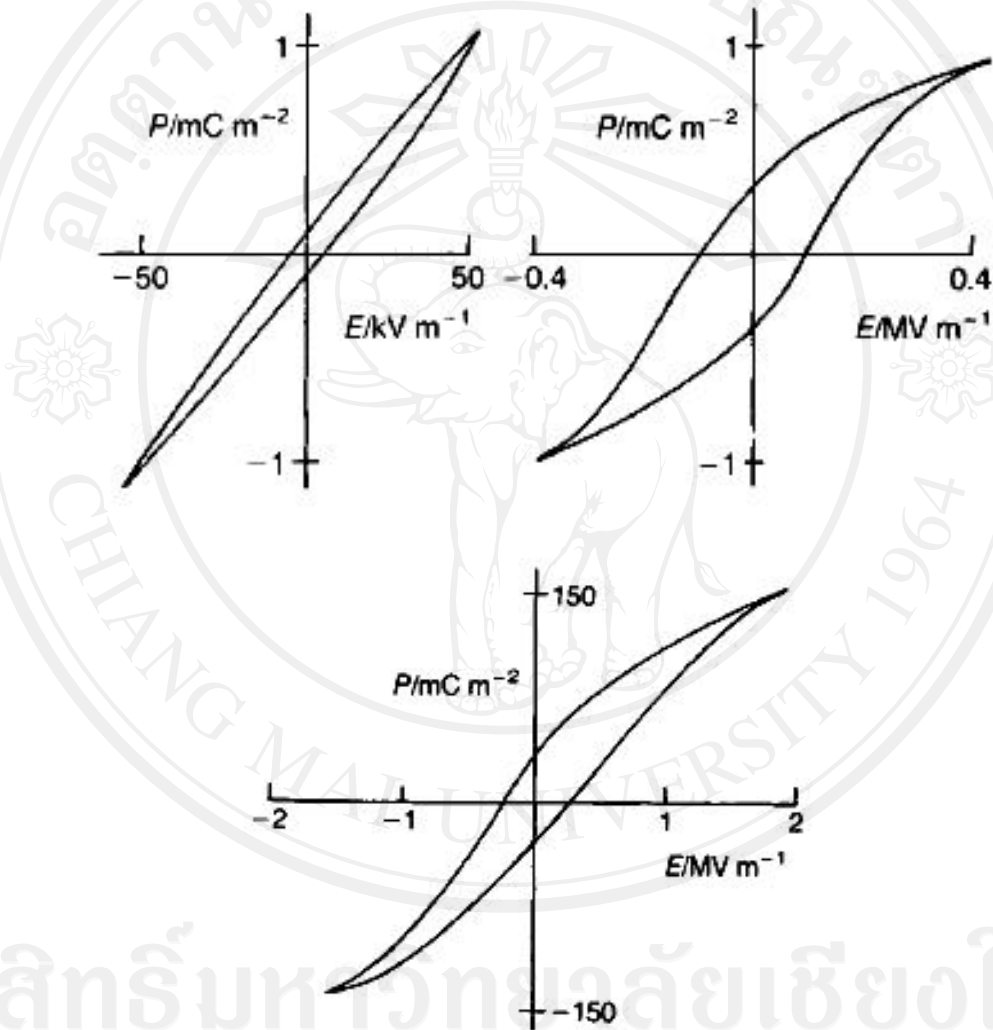
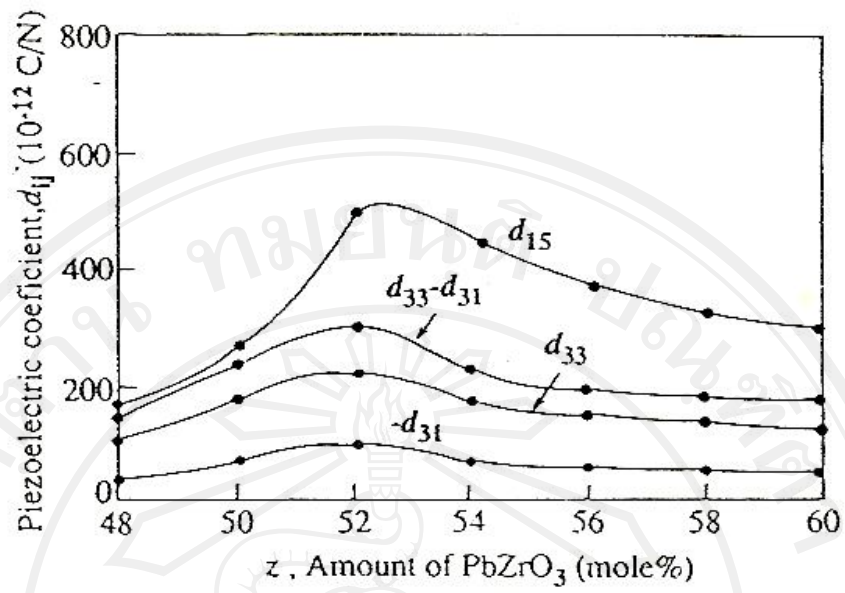
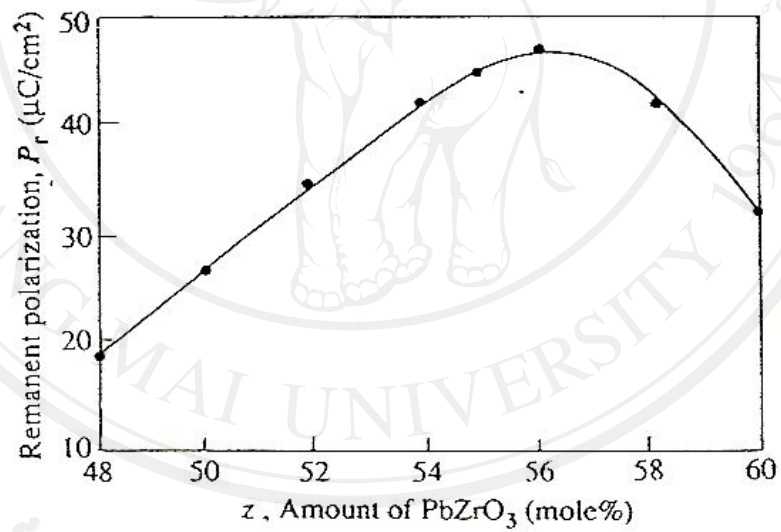


Fig 2.7 P-E loops with increasing peak field strengths at 50 Hz for a ceramic ferroelectric [28]



(a)



(b)

Fig 2.8 (a) variations, at room temperature of piezoelectric coefficient d_{ij} and (b) remanent polarization P_r with composition of PZT near the morphotropic phase boundary [18]

2.2 Organic ferroelectric materials

In the beginning of the 1960s, piezoelectricity in synthetic organic polymer was discovered and initially they were mainly synthetic biological materials, such as polypeptides. Among these synthetic polymer, those with easily stretchable and polarizable structures such as polyvinylidene fluoride (PVDF, or PVF₂, which is also ferroelectric) films, began to attract special attention from researchers, and it seems now that many polymer films exhibit piezoelectric properties. Several piezoelectric devices made of PVDF films, including underwater ultrasonic transducers and electroacoustic transducers (such as microphones, earphones, loudspeakers, pick-up heads), were quickly developed after the initial discovery.

The ferroelectric and the piezoelectricity in the β phase of the polyvinylidene fluoride were observed in the mid-seventies. Due to its high pyroelectric constant it has been widely used in pyroelectric detectors. It was also discovered in the 1970s that several smectic liquid crystals possess ferroelectricity. At present there are many applications in which the electrooptic properties of liquid crystals are exploited. Most of these applications involve switching of their optical properties by an external electric field.

Since enhanced piezoelectricity has achieved for PVDF in the 1970s piezoelectric composites composed of PZT powder in an α -phase PVDF matrix have been developed. This composite of piezoelectric ceramic/PVDF has both the softness of a polymer and the high piezoelectricity of ceramics [27].

2.2.1 Polyvinylidene fluoride films

At present we understand that many polymer films exhibit piezoelectric properties, although they are derived from different mechanisms. The values of the piezoelectric coefficient for different polymer films extend over three orders of magnitude; the highest value of about 20×10^{-12} C/N is observed in these cases of stretched and polarized Polyvinylidene fluoride films, as can be seen from Table 1 [32].

2.2.2 Structure and piezoelectricity of PVDF

Among the polymers listed in table 2.1, polyvinylidene fluoride (PVDF) with the chemical formula of $[\text{CH}_2\text{CH}_2]_n$ is a popular piezoelectric and pyroelectric material.

Table 2.1 Piezoelectric and pyroelectric coefficients of polymer films at room temperature [27]

Polymer	d_{33}	d_{32}	d_{31}	d_{14}	ρ
	(10^{-13} C/N)				$(10^{-9} \text{ C/cm}^2\text{K})$
PVDF (phase β , polarized)	32	5-20	20-200	0	-2 - -4
PFV (polarized)	-	-	10-13	0	-1.0
PCV (polarized)	-	-	5-13	0	-0.4
PVDF (phase α , polarized)+PZT (80 wt.%)	-	170	170	0	-
Poly- γ -benzyl α -glutamate (α helicoidal)	0	170	0	-40	-
Poly- γ -methyl α -glutamate (α helicoidal)	0	0	0	-27- -50	-
Cellulose triacetate	0	0	0	-1	-
Poly-D-propylene oxide	0	0	0	-0.2	-

The piezoelectric and pyroelectric properties of polyvinylidene fluoride arise primarily from the remanent polarization that can be attained by the orienting the dipoles in the crystalline phase of the polymer in the strong electric field [33, 34].

The microscopic mechanisms and the physical basis of piezoelectricity in PVDF have been proposed by Broadhurst and Davis [35]. PVDF crystallizes from the melt into spherulitic structures. The volume fraction of crystalline material is typically about 50%, depending on the thermal history. Most of the uncrystallized molecules are in a metastable liquid phase.

The glass transition temperature for this liquid phase is around -50°C . The spherulites consist of lamellae that grow outward from the common center during crystallization. These lamellae are typically 10-20 nm thick, depending on the conditions of crystallization. The molecular chains are approximately normal to the large lamellae surfaces and to the radii of the spherulites. Much of the liquid material is probably located between the crystal lamellae.

A typical region is shown schematically in Fig. 2.9. It consists of parallel layers of alternating crystal and liquid material, each layer of the order of 10-20 nm thick. Since the molecular lengths are of the order of 100 times the lamellae thickness, each molecule may pass many times through one or more of the crystal layers and it free to assume flexible and irregular configurations in the liquid layers.

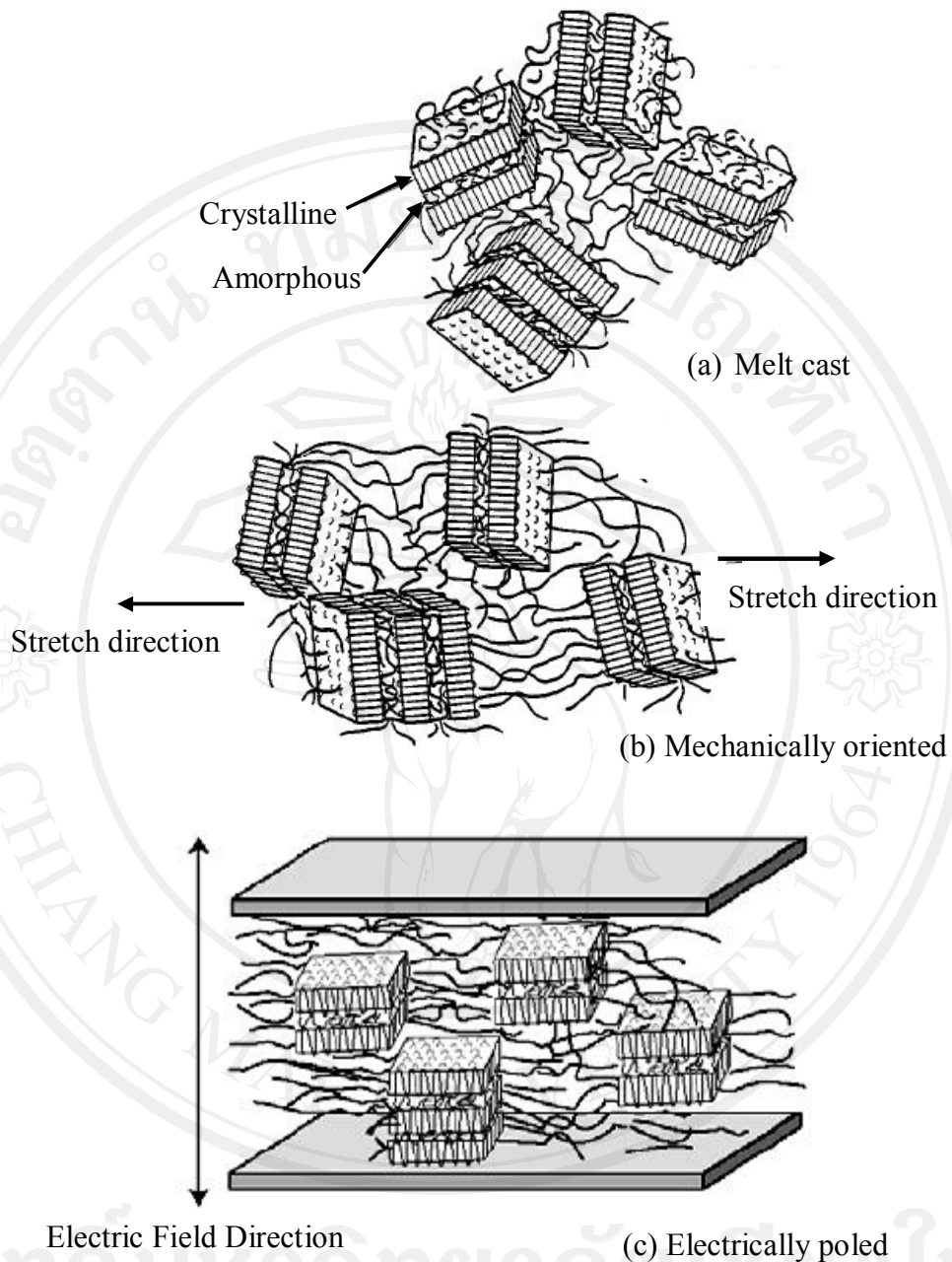


Fig 2.9 Schematic illustration showing random stacks of amorphous and crystal lamellae in PVDF polymer. Figure (a) represents the morphology after the film is melt cast; (b) is after orientation of the film by mechanically stretching to several times its original length; (c) is after depositing metal electrodes and poling through the film thickness [35]

PVDF is inherently polar. The hydrogen atoms are positively charged and the fluorine atoms are negatively charged with respect to the carbon atom in the unit $[\text{CH}_2\text{CF}_2]_n$ of the polymer. In the liquid phase, the molecules continually change shape due to rotations about the carbon-carbon bonds. The average dipole moment of a group of molecules in a liquid region is zero in the absence of an electric field because of the random orientations of individual dipoles. A film of PVDF quenched, after melting, at a temperature below 150°C crystallizes in phase α (or form II), which has a 2_1 helical structure and the resulting conformation is close to trans-gauche-trans-gauche (*tg₂g*) [36]. As a result of a stretching at about 60°C the α -phase film undergoes transition to the β -phase (or form I), which has to a large extent an all-trans (*ttt*) conformation ordered in such a way as to give rise to spontaneous polarization [37]. The amount of β -phase in PVDF film depends on the temperature and the elongation [38]. Fig.2.10 shows an elementary cell of PVDF crystal structure in β phase [39-41].

The cell belongs to the space group $Cm2m$ and the dipole moments of two chains in the elementary cell are oriented parallel to the b -axis. Such an arrangement of the dipole moments has a high value of spontaneous polarization $P_s = 13 \mu\text{C}/\text{cm}^2$ [41]. A PVDF film in β phase, polarized at elevated temperatures, shows very strong piezoelectric and pyroelectric properties. However, a polarized α -phase film does not show these properties to that extent. The third structure variety, similar to the phase β , can be obtained by crystallizing polyvinylidene fluoride melted at about 179°C , or in the course of solution crystallization [42].

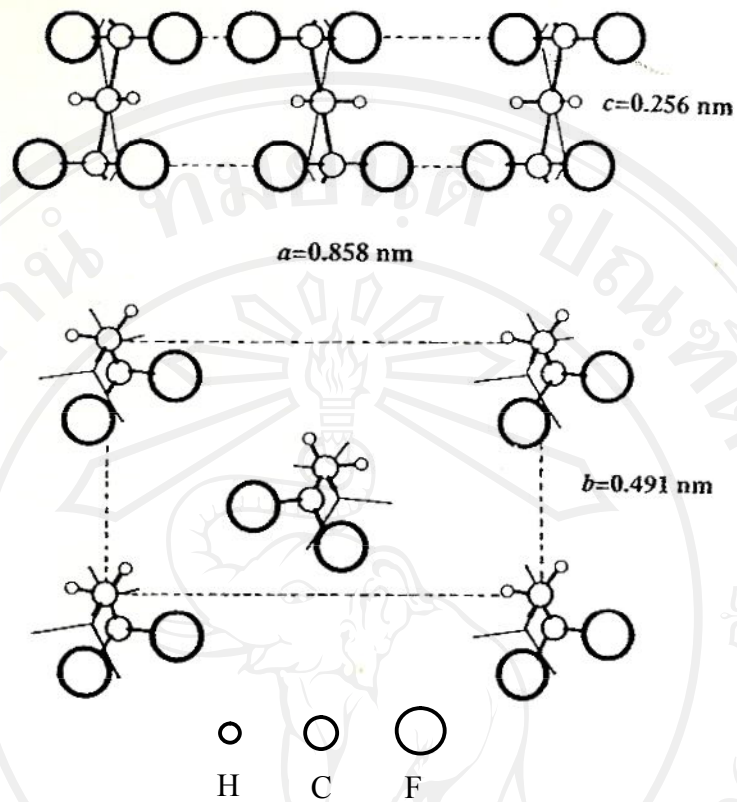


Fig 2.10 Elementary cell of the PVDF crystal structure in phase β [39]

This structure is known as the phase γ (or form III). It has been found that [43] the transition from the unoriented phase C to the oriented phase β induced by stretching at 150°C occurs simultaneously with the transition from spherulitic to fibrillar form. By poling the α form at high electric fields, another phase α_p (form IV, or phase δ) can be formed [44]. The cross-sectional views of these conformations (i.e., as viewed from above down the molecular chain) are shown in Fig.2.11. All the four crystal structures are stable (or metastable) at room temperature and three have polar unit cells. Thus, a crystal in all α_p (polar α), β and γ phases has a net dipole moment.

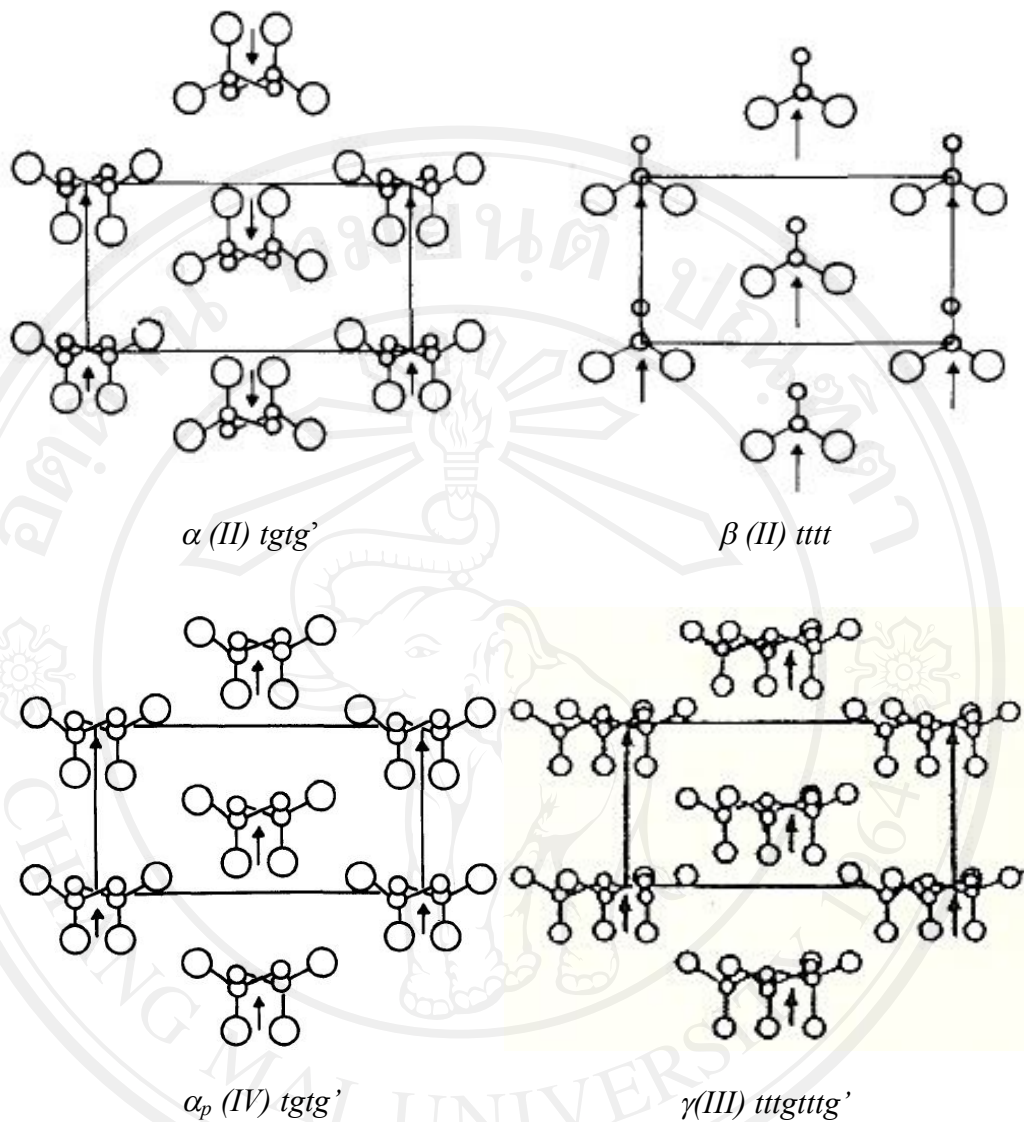


Fig 2.11 Projections of four crystal structures of PVDF viewed along the molecular axes. Dipole moments are shown by arrows. Large circles represent fluorine atoms, small circles represent carbon atom; hydrogen atom are not shown [35]

A phase transformation in PVDF crystal can occur due to mechanical stretching, high-temperature annealing or application of electric fields. In addition to phase changes, changes in the orientation and phase occur by rotations about the carbon-carbon bonds, or by rotation of molecular segments about their long axis, or both. The

dipole alignment occurs by rotation of the molecular segments within the crystal phase about the molecular chain axis (i.e., the $1'$ –axis in Fig. 2.12).

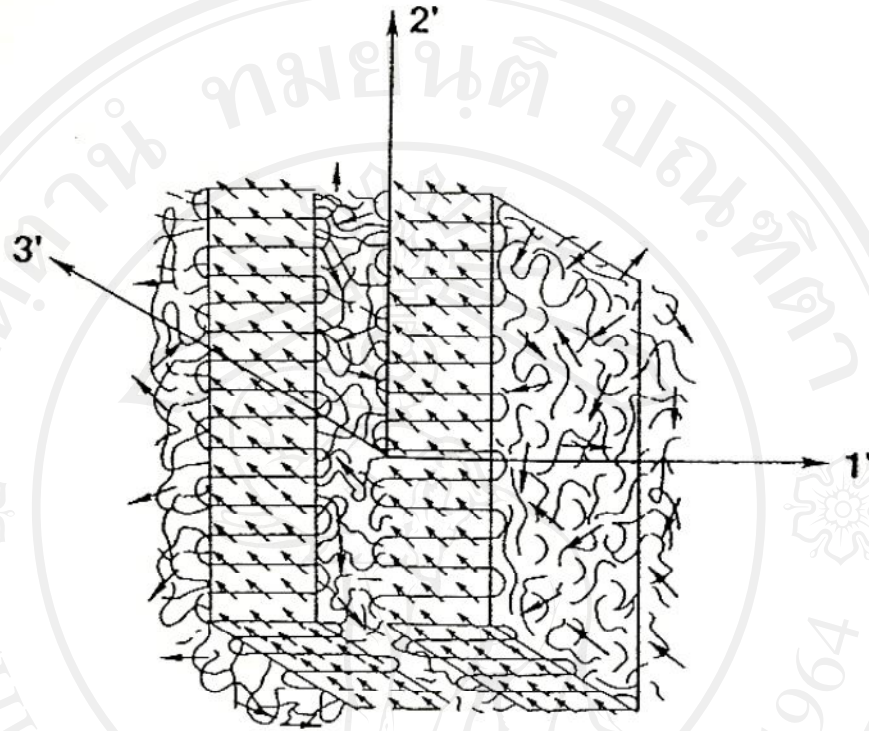


Fig 2.12 Schematic picture of a liquid-crystal stack showing the chain and dipole directions in the crystals [34]

The poling of the crystal is, therefore, best done when the molecular segments are normal to the poling field, i.e., in the plane of the film. The processing of the PVDF film usually consists of extrusion followed by stretching or rolling which tends to align the $1'$ –axis of the crystal parallel to the stretching direction, giving the crystals the desired orientation. It also breaks up the spherulites, and converts them into irregularly shaped but preferentially aligned stacks of alternating layers of liquid and crystal material, as shown in Fig 2.9 (b). It appears reasonable to assume that the field is more effective in aligning the dipoles during the time the mechanical

processing is reforming the crystals in spherulitic form into orientated lamellae. This idea has led to several processing schemes which combine simultaneous poling with stretching [45], rolling or extrusion.

2.3 Portland cement

2.3.1 Portland cement: general

Portland cement is manufactured from lime in the form of chalk or limestone and silica and alumina in the form of clay or shale. Since, they are the most widely used, subsequent discussion will be concerned entirely with Portland cement systems. When anhydrous cement as a dry powder is mixed with water, a cement paste is formed. A relatively slow chemical reaction or hydration process occurs between cement and water resulting in the formation of new compounds which bind the aggregates together into a coherent solid mass. The cement paste remains in a plastic or *fresh state* for up to about four hours after mixing the cement and water together, enabling the concrete (concrete is a mixture of naturally occurring gravels or crushed rock materials call *aggregates* bonded together by some form of *cement*) to be compacted and moulded in to the desired shape. As the hydration process continues, the cement paste and subsequently stiffen into the final *hardened state* [46].

The structure of fresh and hardened cement pastes, mortars (mortar is a mixture of sand and cement), and concretes are complex in the extreme. There is an almost infinite range of possible compositions of anhydrous cement compounds, of amounts of water in cement paste, of types and particle size distribution of aggregates and of volume fractions of manufacture. Furthermore, the structure and properties of

hardened cement paste are still not completely established [46]. Hydration process of cement paste is a very important process.

2.3.2 Compound composition of anhydrous Portland cement

The anhydrous compounds that form Portland cement are the result of a partial solid state reaction involving mainly lime on the one hand and silica, alumina and ferric oxide on the other. In principle 75% limestone or chalk and 25% clay or shale are blended into an intimate, finely divided mixture (particle size less than 100 micron), which is heated gradually in inclined rotary kilns to 1450°C when a series of reactions take place and partial melting finally occurs. On cooling, the compounds clinker together and Portland cement is produced when this clinker, with a small percentage of gypsum ($\text{CaSO}_4 \cdot 2\text{H}_2\text{O}$), is ground to a fine powder having a particle size of about 1-100 micron.

The oxide and potential compound compositions of typical Portland cements are shown in Table 2.2 [47]. The four major compounds in Portland cements have compositions approximating to tricalcium silicate C_3S , dicalcium silicate C_2S , tricalcium aluminate C_3A and tetracalcium aluminoferrite C_4AF . The percentage of these compounds have been calculated from the oxide content by the Bogue formulae [48] which assume that the four major compounds and the equilibrium is reached at the clinkering temperature. Small variations in the lime content cause large alterations in the C_3S and C_2S content of cements.

The presence of an excess of uncombined or free lime must be avoided in cement clinker, since it undergoes an increasing in volume during hydration, so weakening the hardened paste. Other minor components to be found in cement clinker

in small quantities include magnesium oxide and the alkaline oxides K_2O and Na_2O . These oxides affect the idealized compound structure and hydraulic properties of cements to an extent which has yet to be determined.

Table 2.2 Typical oxide and compound compositions of Portland cements [47]

	Symbol	Ordinary %	Rapid hardening %	Sulphate resisting %	
Oxides	CaO	C	63.1	64.5	60.9
	SiO ₂	S	20.6	20.7	21.2
	Al ₂ O ₃	A	6.3	5.2	4.0
	Fe ₂ O ₃	F	3.6	2.9	6.6
	MgO	M	0.8	1.3	0.9
	Na ₂ O	N	0.3	0.1	0.3
	K ₂ O	K	0.6	0.7	0.7
	SO ₃	S	2.6	2.7	2.2
	TiO ₂	T	0.4	0.3	0.3
Compounds	C ₃ S		39	50	40
	βC ₂ S		30	21	31
	C ₃ A		11	9	0
	C ₄ AF		11	9	20
	Free Lime		1.7	2.0	0.9

2.3.3 The hydration of Portland cement

The anhydrous cement compounds, when mixed with water to form pastes, produce unstable saturated lime solutions from which the hydration products are gradually deposited by an exothermic reaction. When they are hydrated separately,

the four major compounds produce their own reaction products and gain strength at different rates (see Fig. 2.13[49])

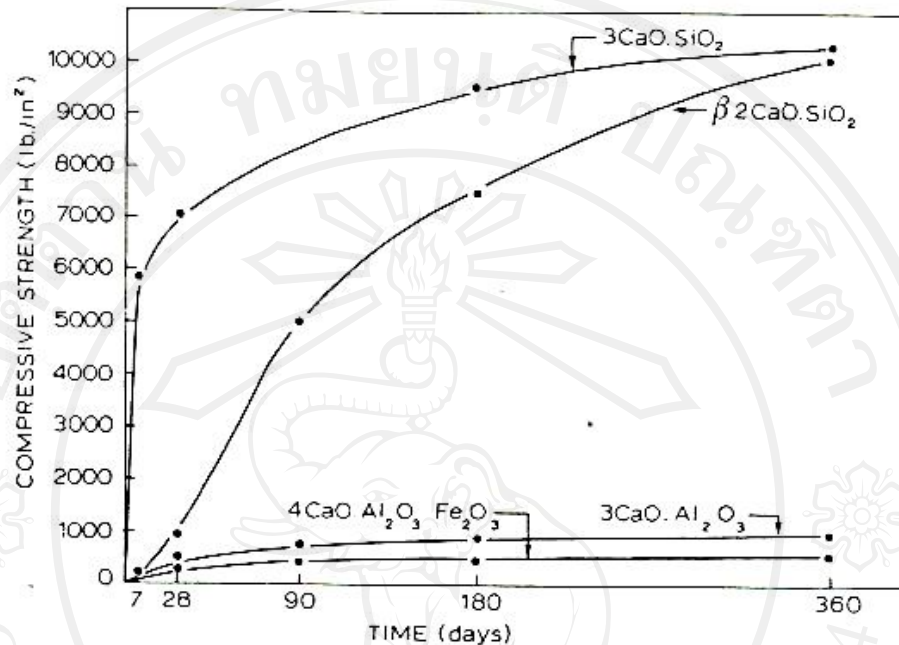


Fig 2.13 The strength developed by Portland cement compounds. [49]

Tricalcium silicate C_3S has all the attributes of Portland cement. When finely ground and mixed with water, it hydrates quickly and crystals of calcium hydroxide $Ca(OH)_2$ are rapidly precipitated. Around the original grains, a gelatinous hydrated calcium silicate is formed which, being impermeable, slows down further hydration considerably. Hydrated C_3S sets or stiffens within a few hours and gains strength very rapidly, attaining the greater part of its strength within one month [46].

Beta dicalcium silicate βC_2S , the hydraulic form of C_2S , exhibits no definite setting time, but does stiffen slowly over a period of some days. It produces little strength for about fourteen days, but after one year its strength is equal to that of C_3S .

The greater reactivity of C_3S can be attributed to the more open structure of the crystal lattice of C_3S compared with the denser packing of the ion in βC_2S [50]

Tricalcium aluminate C_3A reacts very rapidly with water and the paste sets almost instantly with the evolution of so much heat that it may dry out. The addition of 3-4% to cement clinker, which corresponds to 25-50% of the C_3A content, produces a normal setting time. Hydrated C_3A produces little strength and has a low resistance to sulphate attack [46].

Tetracalcium aluminoferrite C_4AF , or the ferrite phase, reacts quickly with water, but less rapidly than C_3A , and develops little strength [46].

When the four major compounds are mixed together in Portland cement, the presence of gypsum appears to have little effect on the rates of hydration and reaction products of the two calcium silicate compounds C_3S and βC_2S , whereas it affects C_3A and C_4AF considerably. In the presence of a lime and gypsum solution, C_3A produces not only a calcium aluminate hydrate, but also calcium sulphoaluminate compounds, the high sulphate form of which is called *ettringite*. In the case of C_4AF , an analogous sulphoferrite is formed but both of these sulphate compounds have little or no cementitious value.

The retardation of the hydration of C_3A may be due either to the formation of a protective coating of sulphoaluminate around the cement particles, or to the impermeable nature of the coating of the hydrate calcium silicate [51]. Whatever the reason, there is a marked slowing down of the hydration process to give a *dormant period* [51] which may last an hour or so after initial mixing. The end of the dormant period is marked by an increase in the rate of hydration and as more calcium silicate

hydrate (CSH) is formed the cement paste gradually stiffens and hardens. Subsequent strength development depends on the continued hydration of C_3S and βC_2S .

2.3.4 Rate of hydration

There are many factors that affect the rate of hydration of the various phases in cement, and no two samples of cement will behave in an identical manner. The reactivity of the phases is dependent on such factors as the mean particle size and particle size distribution. These, in turn, are dependent on the degree of grinding of the clinker, its rate of cooling, the impurities present, the relative amounts of the phases and the interaction between the phases as hydration proceeds [52]. For example, the rate of hydration of C_2S is increased in the presence of C_3S due to changes in the concentration of Ca^{2+} and OH^- in the solution from the hydration of the C_3S . The rates of hydration of the other components are also interconnected. However, in general, the rates of reaction will be in the order $C_3A > C_3S > C_4AF > C_2S$. This is indicated by the depth of hydration product formed after six months on 30-55 μm grains of each phase in Table 2.3.

Table 2.3 Depth of hydration product (μm) on 30-55 μm grains [53]

	3days	7days	28days	6 months
C_3A	10.7	10.4	11.2	15
C_4AF	7.7	8.0	8.4	13.2
C_3S	3.5	4.7	7.9	15.0
C_2S	0.6	0.9	1.0	2.7

2.3.5 Volume change during hydration

One of the characteristics of Portland cement is that there is very little change in total volume as the cement/water mixture sets. This is because the hydration products are less dense than the unhydrated compounds and fill the volume that was previously occupied by both the water and the unhydrated compounds. It should be noted that the hydration reactions continue long after the cement has set and it is here that the difference in the hydration behavior of the compounds becomes important [54].

The grain of the major components, C_3S and C_2S , will continue to hydrate after the cement has set, but the hydration products will only occupy the space available for them, that is, the volume occupied by the water with which they are reacting. As soon as this volume is filled with reaction products, the reaction ceases [54].

However the hydration products of the minor components, C_3A and C_4AF , continue to be formed even when there is insufficient space and the hydration of these compounds results in an expansion of the paste volume. If the paste has already hardened, then the hydration of these compounds results in a build-up of stress in the set cement which will cause cracking. This is why the addition of the correct amount of gypsum to the cement paste is critical. If too little is added then a flash set will occur. If the correct amount is added, then the expansion caused by the hydration of C_3A will take place before the cement has set, and no damage is done, but if too much gypsum has been added, then ettringite will continue to be formed after the cement has set and cracks are then formed. It should be emphasized here that C_3A and C_4AF are minor constituents in the cement and therefore the net expansion that takes place when they hydrate is small, and as will be seen later, this can be put to advantage to counteract the drying shrinkage of the cement [54].

The amount of water theoretically required to hydrate the cement paste completely is about 0.25 times the mass of the cement. If this amount is used it is found that there is still some unreacted cement. This is because some of the water becomes adsorbed in the pores between the gel particles (gel pore) and is therefore not available for reaction with the cement. In reality, in order to get complete hydration a water/cement ratio of about 0.38 has to be used in the mix[54].

2.3.6 Summary of the hydration of Portland cement

It is the formation of CSH which gives the cement its strength. The laths and needles formed due to the reactions of C_3A and C_4AF result in the initial set of the cement, but these do not contribute significantly to the long-term strength.

C_3S forms CSH much more rapidly than C_2S ; therefore cement with a higher proportion of C_3S will develop strength more rapidly than cements with less C_3S . While it is agreed that the formation of CSH gel is the major factor which contributes to the strength of cement, the role of the CH platelets is still uncertain. The rates of hydration are important; C_3A , C_4AF and C_3S all hydrate rapidly, but C_3S is responsible for the major part of the early strength developed. C_2S hydrates more slowly, and it is this that gives the cement its increase in strength over the long term. It is the hydration of C_3S and C_3A that is responsible for most of the heat evolved in the cement in the first 48 hours. Therefore if this heat evolution is to be limited, C_3A and C_3S should be reduced (this involves a corresponding increase in C_2S , which results in a reduction in early strength but not in the ultimate strength of the cement) [54].

2.3.7 Aggregate and the aggregate/cement bond

The cement serves to bond the aggregate particles together and the nature of the interface between the aggregate and the cement is of great importance. The interfacial region between the aggregate and the cement is through to be very different from the bulk cement regions both in terms of morphology, density and composition [55]. These regions are normally lower in density than the hydrated cement matrix and contain large orientated hexagonal crystals of CH and needle of AF_t . The structure is shown schematically in Fig. 2.14 [55]. This thickness of this interfacial region is about $50\mu\text{m}$, with the weakest part of the zone lying about 5 to $10\mu\text{m}$ away from the interface. The existence of this porous region can affect the fracture characteristics of the concrete and be a factor that limits the strength of the concrete.

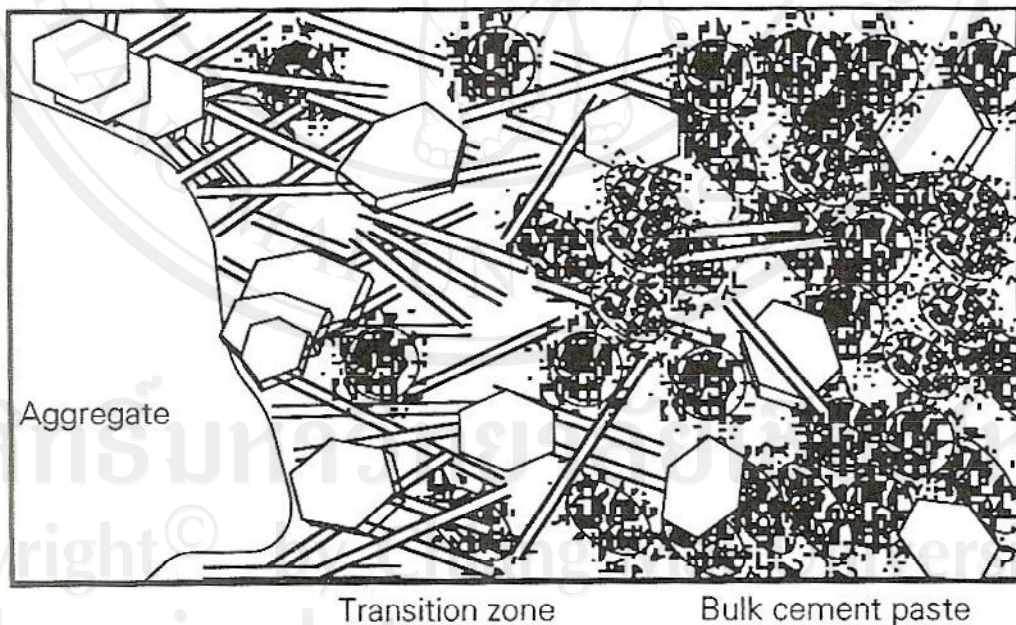


Fig 2.14 The interface between the aggregate and cement paste [54]

Some idea of the quality of the bond between the aggregate and cement can be obtained by inspecting a fractured sample of concrete. Ideally, there should be some fractured aggregate and some pull out. If all the aggregate has fractured, then the aggregate is too weak, and if all the aggregate has pulled out, then either the bond between the cement paste and the aggregate is too weak or the cement paste itself is too weak [54].

2.3.8 Aggregate particle characteristics

Ideally, in mixed concrete, each piece of aggregate (large or small) should be totally surrounded by cement, and the packing of the particles should be as dense as possible. The grading of the aggregate (the section of the particle size ranges to be used and the amount of aggregate in each range) should be such as to give the maximum density of particles packing which minimizes the amount of the more expensive cement used in the mix [54].

Aggregate shape, Surface texture, Porosity and Grading of the aggregate

The relative quantities of coarse and fine aggregate needed to give dense packing will depend on the shape of the aggregate particles. If the aggregate is angular, then the relative proportions of coarse/fine will be different than if it is rounded (spherical), because the random packing of coarse non-spherical particles result in a greater volume of void than the packing of coarse spherical particles and the void need to be filled by fine particles[54]. On the other hand, angular aggregates will produce concrete of a greater strength than spherical aggregates. This due to the

greater surface area/volume ratio of angular aggregates which produces a larger bonding interface between the aggregate and the cement [54, 56].

The *surface texture* of the aggregate is also important, a rough texture results in better bonding because of the larger surface area of the aggregate in contact with the cement. The absorption of water by the aggregate must be taken into account when designing a concrete mix, because if dry porous aggregate is used it will absorb water during the mixing of the concrete and lead to a reduction in the amount of water available to hydrate the cement.

The aim in the *grinding of the aggregate* is to minimize the void space between the aggregate, since this has to be filled with the cement. The selection of the relative amounts of the coarse and fine grades of aggregate is depending on many factors, which include the maximum size of the aggregate, the shape of the aggregate, the size distribution of the coarse and fine fractions, the workability required, the surface texture of the aggregate, the water/cement ratio to be used and the required strength of the concrete [54].

2.4 Carbon graphite

Carbon is an element that exists in various polymorphic forms, as well as in the amorphous state. This group of materials does not really fall within any one of the traditional metal, ceramic, polymer classification schemes. However, it has been decided to discuss these materials in this chapter since graphite, one of the polymorphic forms, is sometimes classified as a ceramic. This treatment focuses on the structures of graphite. The characteristics and current and potential uses of this material are discussed [57].

Graphite

Graphite has a crystal structure (Fig. 2.15) distinctly different from that of diamond and is also more stable than diamond at ambient temperature and pressure. The graphite structure is composed of layers of hexagonally arranged carbon atoms; within the layers, each carbon atom is bonded to three coplanar neighbor atoms by strong covalent bonds. The fourth bonding electron participates in a weak van der Waals type of bond between the layers. As a consequence of these weak interplanar bonds, interplanar cleavage is facile, which gives rise to the excellent lubricative properties of graphite. Also, the electrical conductivity is relatively high in crystallographic directions parallel to the hexagonal sheets.

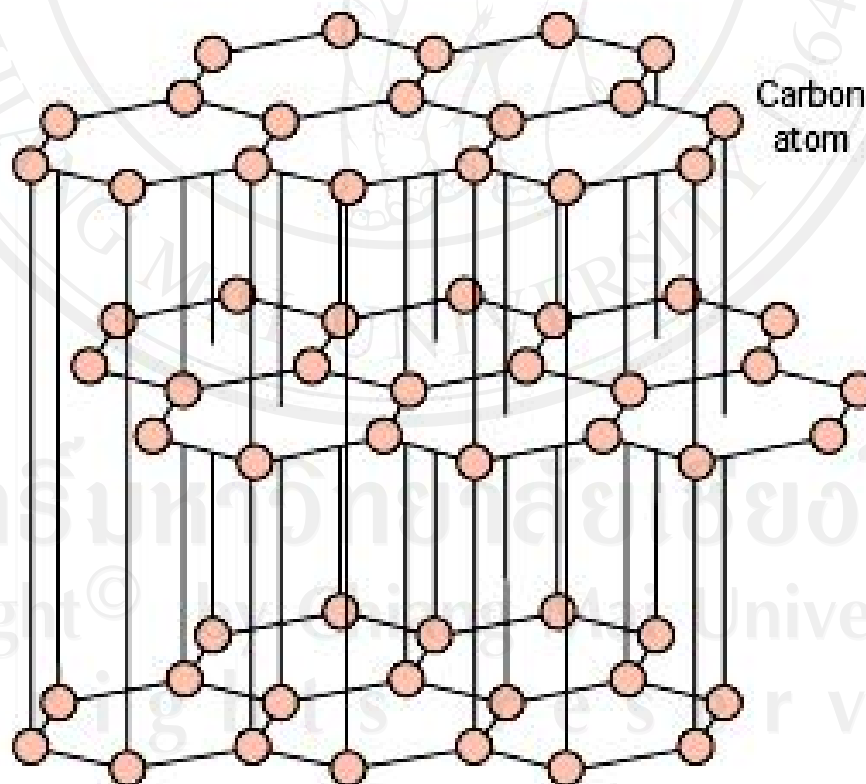


Fig 2.15 The structure of graphite [57]

Other desirable properties of graphite include the following: high strength and good chemical stability at elevated temperatures and in nonoxidizing atmospheres, high thermal conductivity, low coefficient of thermal expansion and high resistance to thermal shock, high adsorption of gases, and good machinability. Graphite is commonly used as heating elements for electric furnaces, as electrodes for arc welding, in metallurgical crucibles, in casting molds for metal alloys and ceramics, for high temperature refractories and insulations, in rocket nozzles, in chemical reactor vessels, for electrical contacts, brushes and resistors, as electrodes in batteries, and in air purification devices [57].

2.5 Composite materials

Composite materials have found use in a number of structural applications, but their use in the electronics industry surprisingly widespread. Such applications and advantages of composites electroceramics include their use in piezoelectric transducers, sensors, and actuators. Functional composites make use of a number of underlying the basic ideas, including the following: sum and product properties, connectivity patterns and percolation threshold. An important approach to making functional composites is to bring together two or more different materials, each of which has a phase transition associated with it [58].

In most electronic devices there are several phases involved and a number of material parameters to be optimized. An electromechanical transducer, for example, may require a combination of properties such as large piezoelectric coefficient (d or g), low density and mechanical flexibility.

In general, the task of materials design may be considerably simplified if it is possible to devise a figure of merit which combines the most sensitive parameter in a form allowing simple intercomparison of the possible “trade offs” in properties coefficients. Moreover, for such an application a composite material combining the desirable properties of two different phases might be vastly superior. The main problem is to effect the combination in such a manner as to exploit the desirable features of both components and thereby maximize the figure of merit [1, 11].

Combining materials mean not only choosing component phases with the right properties, but also coupling them in the best manner. Connectivity of the individual phases is of utmost importance, because this controls the electric flux pattern as well as the mechanical properties. Symmetry is a second important consideration, since symmetry and properties are interrelated through tensor coefficients. In this regard there are several levels of symmetry to be considered: the crystallographic symmetry of each phase, the symmetry after processing, the combined symmetry of the composite, and the environmental influence on the total symmetry including electrodes and clamps [1, 11, 58].

The points of interest are schematically formalized in Fig. 2.16 for a simple two-phase system. It is interesting to note that in some composites, not only are the properties of the separate phases modified (sum properties), but the composite may exhibit completely new couplings (production properties) not found in the separate phases.

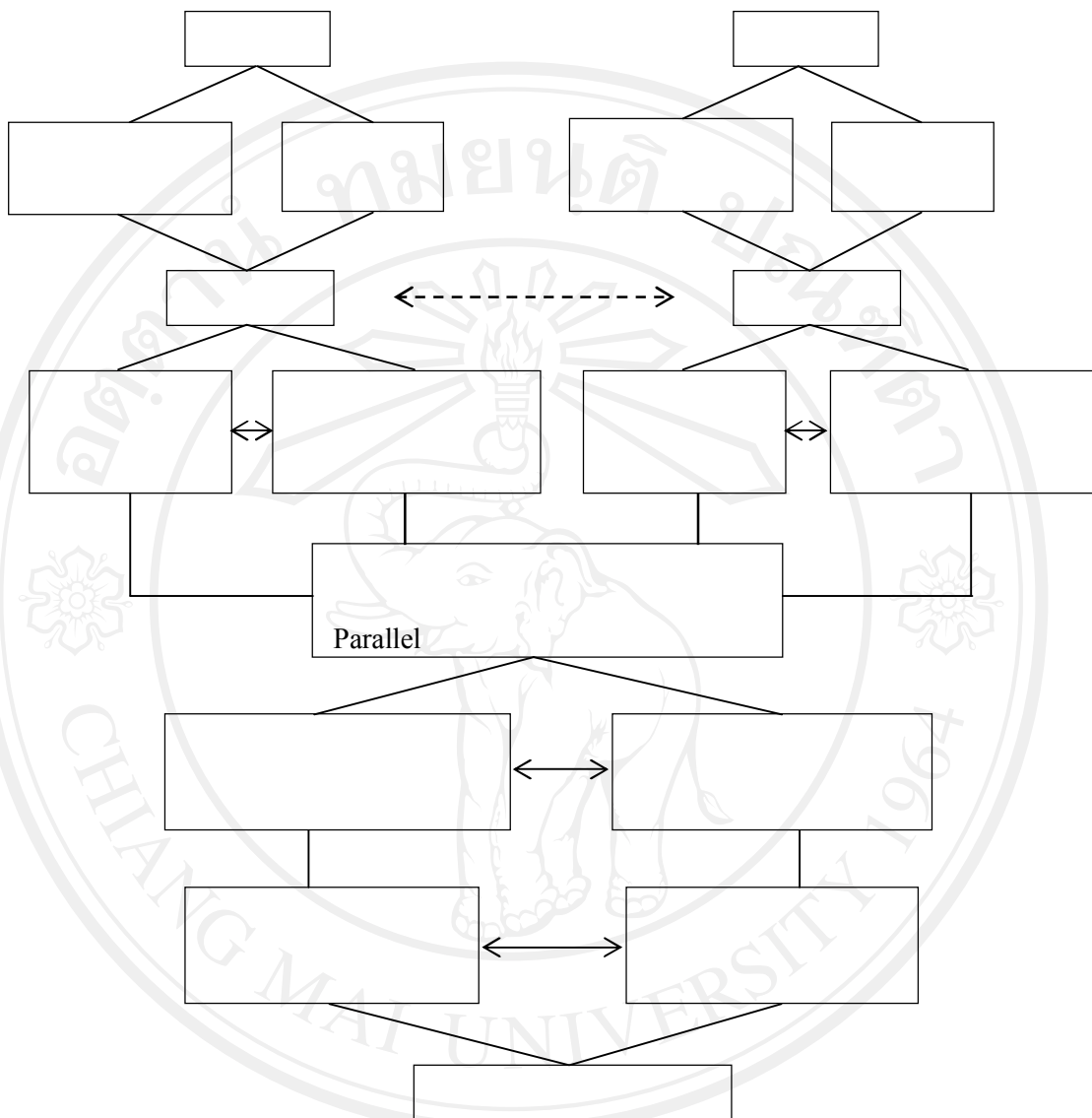


Fig 2.16 Chart illustrating design considerations for optimizing the performance of solid state devices. The task of the materials engineer is to find the materials, processing methods, and connectivity patterns which maximize the figure of merit [11]

2.5.1 Properties of composite materials

The physical and chemical properties of composites can be classified as sum properties, combination properties, and product properties. The basic ideas underlying sum and product properties were introduced by van Suchtelen [59].

For *sum property*, the composite property coefficient depends on the corresponding coefficients of its constituent phases. Thus the stiffness of a composite is governed by the elastic stiffnesses of its component phases and the mixing rule appropriate to its geometry. In general, the property coefficient of the composite will be between those of its constituent phases. This is not true for *combination properties*, which involve two or more different coefficients. Poisson's ratio is a good example of a combination property since it is equal to the ratio of two compliance coefficients. Some composite materials, e.g. wood [60], have extremely small Poisson ratios, even smaller than those of the materials used to make the composite. *Product properties* are more complex and more interesting. The product properties of a composite involve different properties in its constituent phases; the interactions between the phases often causing unexpected results [58].

Sum properties

The dielectric constant will be used to illustrate a simple sum property. Series and parallel mixing rules delimit the bounding conditions for the dielectric constant \bar{K} of a diphasic composite:

$$\bar{K}^s = V_1 K_1^s + V_2 K_2^s + \dots \quad [58] \quad (2.6)$$

where K_1 and K_2 are the dielectric constants of the constituent phases, and V_1 and V_2 are their volume fractions. The exponent n is + 1 for parallel mixing and -1 for series mixing. For many composites, the geometric arrangement is partly series and partly parallel, in which case \bar{K} can often be described by a logarithmic mixing rule for which the exponent $n \sim 0$. There are, of course, many other mixing rules in addition to the series and parallel models. These represent only the limiting conditions. A more complete discussion of the dielectric properties of heterogeneous materials is given in the classic article by van Beek [61].

Combination properties

For simple mixing rules the properties of a composite lie between those of its constituent phases, but combination properties involve two or more coefficients which may average in a different way.

For example, acoustic wave velocity determines the resonant frequency of piezoelectric devices. The velocity of waves propagating along the length of a long, thin rod is

$$v = (E/\rho)^{1/2} \quad [58] \quad (2.7)$$

where E is Young's modulus and ρ is the rod's density. Fiber-reinforced composites often have very anisotropic wave velocities. Consider a compliant matrix material reinforced with parallel fibers. Long, thin rods fashioned from the composite have different properties when the fibers are oriented parallel or perpendicular to the length of the rod. The wave velocities are much faster for rods with longitudinally oriented (v_L) fibers than for those with transversely oriented (v_T) ones.

Product properties

The interaction of different properties in the two phases of a composite result in yet a third property, a product property. The combination of different properties of two or more constituents sometimes yields surprisingly large product properties. Indeed, in a few cases, product properties are found in composites that were entirely absent in the phases that make up the composite. Table 2.4 list a few of the hundreds of possible product properties [1], including several described in this article.

Table 2.4 Examples of product properties [58]

Property of phase 1	Property of phase 2	Composite product property
Thermal expansion	Electrical conductivity	Thermistor
Magnetostriction	Piezoelectricity	Magnetolectricity
Halle effect	Electrical conductivity	Magnetoresistance
Photoconductivity	Electrostriction	Photostriction
Superconductivity	Adiabatic demagnetization	Electrothermal effect
Piezoelectricity	Thermal expansion	Pyroelectricity

2.5.2 Connectivity

Connectivity is a key feature in property development in multiphase solids since physical properties can change by many orders of magnitude depending on the manner in which connection are made. Imagine, for instance, an electric wire in which

the metallic conductor and its rubber insulation were connected in series rather than in parallel [11].

Each phase in a composite may be self-connected in zero, one, two, or three dimensions. It is natural to confine attention to three perpendicular axes because all property tensors are referred to such system [62]. If we limit the discussion to diphasic composites, there ten connectivities: 0-0, 1-0, 2-0, 3-0, 1-1, 2-1, 3-1, 2-2, 3-2 and 3-3. The ten different connectivities are illustrated in Fig. 2.17, using a cube as the basic building block.



Fig 2.17 Connectivity patterns in a diphasic composite system [63]

Fig.2.17 shows ten connectivity patterns for a diphasic solid. Each phase has zero-, one-, two- or three-dimensional connectivity to itself. In the 3-1 composite, for instance the shaded phase is three-dimensionally connected and the unshaded phase is one- dimensionally connected. Arrow is used to indicate the connected directions.

2.5.3 Piezoelectric composites

To illustrate the major modifications in ensemble properties which can be affected even in sample linear system, one-dimensional solution are presented for the piezoelectric properties of heterogeneous two-phase structures.

Series connection

Consider first the piezoelectric properties of lamellar diphasic composites. Longitudinal piezoelectric coefficient d_{33} has been derived for a diphasic piezoelectric with the constituent phases arranged in alternating layers normal to the x_3 direction (Fig. 2.18(a)). Designating phase 1 with a subscript 1, and phase 2 with a subscript 2, phase 1 has volume fraction v^1 , piezoelectric coefficient d_{33}^1 and permittivity ϵ_{33}^1 , and phase 2 has v^2 , d_{33}^2 and ϵ_{33}^2 , respectively. Solving for the piezoelectric coefficient of the composites gives.

$$d_{33} = \frac{v^1 d_{33}^1 \epsilon_{33}^2 + v^2 d_{33}^2 \epsilon_{33}^1}{v^1 \epsilon_{33}^2 + v^2 \epsilon_{33}^1} \quad [11] \quad (2.8)$$

Using the relation $g_{33} = d_{33}/\epsilon_{33}$ yields the piezoelectric voltage coefficient

$$g_{33} = \frac{v^1 d_{33}^1}{\epsilon_{33}^1} + \frac{v^2 d_{33}^2}{\epsilon_{33}^2} = v^1 g_{33}^1 + v^2 g_{33}^2 \quad [11] \quad (2.9)$$

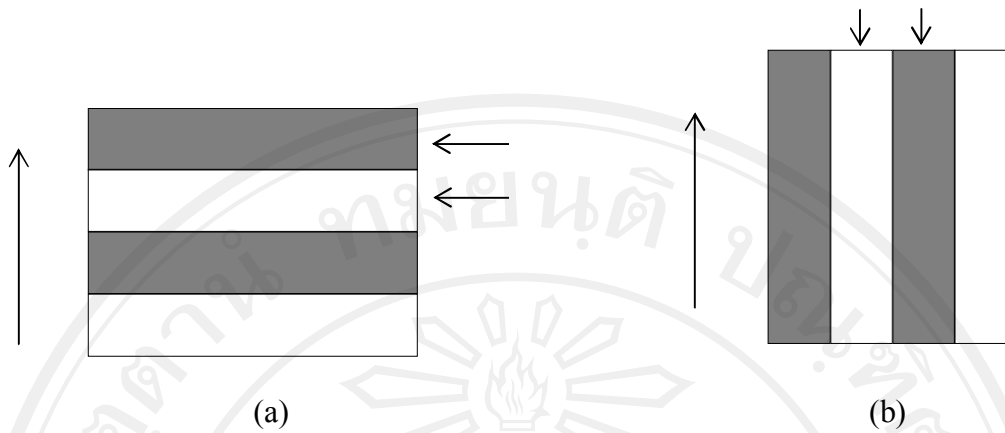


Fig 2.18 The series (a) and parallel (b) model used in estimating the piezoelectric effect of diphasic solid [11]

It is interesting to note that for series connection even a very thin low-permittivity layer rapidly lowers the d -coefficient but has little effect on the corresponding g -coefficient.

Parallel connection

If the two phases lie in layers perpendicular to the electrode (Fig. 2.18(b)), again for the one-dimensional case and neglecting transverse coupling, the composite piezoelectric coefficient is

$$d_{33} = \frac{v^1 d_{33}^1 s_{33}^2 + v^2 d_{33}^2 s_{33}^1}{v^1 s_{33}^2 + v^2 s_{33}^1} \quad [11] \quad (2.10)$$

Where v^1 and v^2 are the elastic compliances for stresses normal to the electrode. For the voltage coefficient,

$$g_{33} = \frac{v^1 d_{33}^1 s_{33}^2 + v^2 d_{33}^2 s_{33}^1}{(v^1 s_{33}^2 + v^2 s_{33}^1)(v^1 \varepsilon_{33}^1 + v^2 \varepsilon_{33}^2)} \quad [11] \quad (2.11)$$

A composite of interest here is that of an elastically compliant non piezoelectric in parallel with a stiff piezoelectric.

2.5.4 Percolation in composites

Many properties of composite materials such as diffusion, electrical conduction, dielectric response as well as elasticity, are intimately related to the geometrical arrangement of the constitutive phases, including the geometry of the respective interfaces. Percolation theory, whose objective is to characterize the connectivity properties in random geometries and to explore them with respect to physical processes, thus provides a natural frame for the theoretical description of random composites [64].

Percolation represents the basic model for a structurally disordered system [65-67]. For simplicity, consider a square lattice, where each site is occupied randomly with probability p or is empty with probability $1 - p$ (see Fig. 2.19). Occupied and empty sites may stand for very different physical properties. For illustration, let us assume that the occupied sites are electrical conductors, the empty sites represent insulators, and that electrical current can only flow between nearest-neighbor conductor sites.

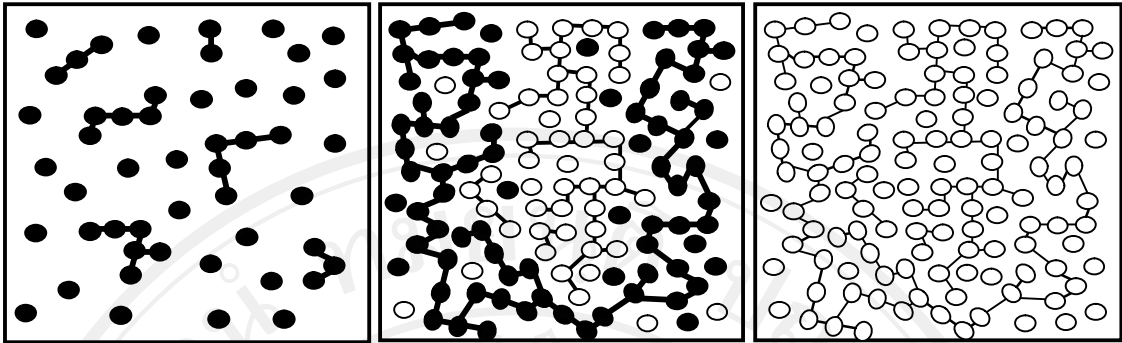


Fig 2.19 Site percolation on the square lattice: The small circles represent the occupied sites for three different concentrations. Nearest-neighbor cluster sites are connected by lines representing the bonds. Filled circles are used for finite clusters, while open circles mark the large infinite cluster [64]

At low concentration ρ , the conductor sites are either isolated or form small clusters of nearest neighbor sites. Two conductor sites belong to the same cluster if they are connected by a path of nearest-neighbor conductor sites, and a current can flow between them. At low p values, the mixture is an insulator, since no conducting path connecting opposite edges of our lattice exists. At large ρ values on the other hand many conducting paths between opposite edges exist, where electrical current can flow, and the mixture is a conductor. At some concentration in between, therefore, a threshold concentration p_c must exist where for the first time electrical current can percolate from one edge to the other. Below ρ_c we have an insulator, above ρ_c we have a conductor. The threshold concentration is called the “*percolation threshold*”, or, since it separates two different phases, the “*critical concentration*”.

Percolation is a well-known phenomenon observed in filler–matrix systems. It is often accompanied by a significant change in certain physical properties within a

rather narrow concentration range [68], such as composites consisting of an insulating polymeric matrix and electro conductive particles. The change in conductivity is explained by formation of a conductive path through the sample when sufficient contacts are created between conductive particles, corresponding to the percolation threshold. The percolation concentration depends on many parameters such as the physical nature of the filler (e.g., surface area, aggregation and shape), chemical composition of the surface, and processing conditions [69].

2.6 Requirement and background of piezoelectric-cement based composites

The development of modern civil engineering, the vibration control and the health monitoring of structures is being introduced [3, 6, 7]. The structural vibration controlling systems and structural health monitoring can provide instantaneous information on a condition of a specified structure also result in a significant increase of safety margin and reductions in maintenance cost. According to different applications, different types of sensors/actuators have been designed and used. It is predicted that the sensors/actuators applicable for application in other engineering fields, such as mechanical engineering but may not be suitable in civil engineering due to the differences in the properties between smart materials and the host structures.

For example, the acoustic impedance, temperature coefficient and shrinkage and creep characteristics of concrete, which is the most popular material in civil engineering, are quite different from those of the metal and alloy which are frequently used in mechanical engineering. The sensors used in mechanical engineering cannot be simply transplanted into the civil engineering applications. Thus a new kind of

sensors/actuators should be developed to meet the requirements of civil engineering applications [7].

As the techniques used in sensors and actuators, piezoelectricity has been proved to be one of the most efficient technologies for most applications in smart structures [70, 71]. And it has attracted great attention in research activities towards the applications of sensors and actuators in civil engineering [27, 72-76]. In all kinds of piezoelectric materials, the piezoelectric composites are especially eminent in different fields. On one hand, they are appropriate more important as the materials for the study of charge transport and energy storage in multi-component systems. On another hand, in applications of various devices there has been a rapid development. In addition, piezoelectric materials can be classified as piezoelectric ceramics, piezoelectric polymers and piezoelectric composites. Many researchers [7, 12, 74] have developed piezoelectric composites by incorporating particles of piezoelectric ceramics into a polymer matrix, such as epoxy, rubber, or some types of piezoelectric polymer, such as polyvinylidene fluoride (PVDF). However, a problem remains in ceramic/polymer piezoelectric composites regarding the difficulty of poling piezoelectric ceramic powders due to the large differences in resistivity and permittivity between polymer matrix and ceramic powders [77].

The most notable application of such composites comprises electromechanical transducer [58, 77, 78]. For example, cement-based PZT ceramic composites are the new developments in sensor/actuator application for concrete structure. Ceramic materials such as barium titanate and Lead zirconate titanate ((PZT) have very good pyro- and piezoelectric properties and as such are used in a variety of application [27, 28]. However, their different mechanical properties limit their use in civil engineering

especially for sensor/actuator (embedded in host structure). Therefore a composite consisting of highly piezoelectric ceramic material combined with cement material would be the ideal replacement to obtain the properties of both these classes.

According to fundamentals of composites, in general a composite is a structural material whose properties are determined by the number of different phases of the material, the volume fractions of the phases, the properties of individual phases, and the ways in which different phases are inter connected [58]. The latter is the most important feature of composites, since the mixing rules of a given property are controlled by the self-connectivity of individual phases [11]. In addition, the preliminary analyses of the feasibility and advanced of cement-based piezoelectric composites regarding acoustic match between them and host material. There is potential for the application of cement-based 0-3 PZT composites in civil engineering because of their better piezoelectric properties and good compatibility with portland cement concrete [7].

In a smart structure, sensor and actuator are essential components for sensing and controlling compared with the achievements in controller design. Moreover, the sensor and actuator suitable for application in the field of mechanical engineering may not be application in civil engineering structures because differences in the properties between a sensor or actuator and the host structures such as acoustic impedance, shrinkage and creep characteristics of concrete. Therefore, new sensor and actuator should be developed to meet the requirements of civil engineering applications [7, 78].

The basic properties of the PZT ceramics, cement paste and concrete are listed in Table 2.5. Moreover, the present work will described new 0-3 piezoelectric ceramic

cement composites that have convenient processibility, a low dielectric permittivity and high piezoelectric charge constant. This combination of properties suggests important applications opportunities, especially for vibration sensors.

Table 2.5 The basic properties of the PZT ceramics, cement paste and concrete

	Vol%	ϵ_r (at 1 kHz)	d_{33} (pC/N)	g_{33} (10^{-3} Vm/N)	ρ (10^3 kg/m ³)	Ref
PZT [7]	100	3643	513	15.9	7.5	[7]
Cement paste	100	~56	-	-	~2.0	[7]
Concrete	100	-	-	-	~2.4	[7]
PZT-PC	50:50	94.2	12.5	15.0	3.73	[79]

For civil engineering applications, piezoelectric PZT-cement based composites have recently been developed for use as sensors in smart structures [7, 78, 80, 81]. The first reported work using piezoelectric PZT to fabricate piezoelectric-cement composites was by Li *et al.* [7, 78, 82, 83]. In 2002, they studied two sizes of PZT ceramic particles mixed with Portland white cement to make the 0-3 piezoelectric composite to investigate the effects of the particle size of PZT on the piezoelectric properties of the PZT/cement composites. Various percent by volume of PZT were mixed and spreaded into Portland cement. Moreover, in 2008 [83] they investigated the nano-PZT powders mixed with white cement. From these works, it can be concluded that ~40-50% by volume is the optimal PZT powder content for acoustic impedance which matched exactly between cement-based piezoelectric composite and concrete.

The piezoelectric properties of the composites increased with the increase of PZT contents. The k_t of the thickness vibration mode and d_{33} were higher than those of the PZT/polymer 0-3 composites and adequate for sensor application. Moreover, it was found that the coarser PZT particles lead to a higher d_{33} in the composites. When the particle size of embedded PZT powder was decreased, the piezoelectric strain factor, dielectric constant and electromechanical coupling coefficient of the PZT/cement composite were all decreased. However, PZT nano-powder was found to give better piezoelectric properties due to the good crystallinity of PZT grains and the network-like distribution of PZT particles in the cement. The all results are showed in Table 2.6 and 2.7, respectively.

Furthermore, Li *et al.* [78] studied the piezoelectric behaviors both theoretically and experimentally of the cement based PZT composites under different poling conditions. Polarizing orientation process was carried out in a silicon oil bath at 160°C. With the aging time after poling process increasing, d_{33} value of cement-based piezoelectric composites increased while d_{33} values of cement/polymer composites showed a decrease trend, the results are shown in Fig 2.20. In 2004, Shifeng *et al.* [80] studied the influences of poling conditions, particle size and contents of PZT on the piezoelectric properties of composites. The specimens were put in a curing room with a temperature of 20°C and relative humidity of 100% for 3 days before measurements. The poling was carried out in a stirred silicone oil bath. In each kind of piezoelectric composite, the contents of PZT were 60, 70, 80 and 85 wt%. The result showed that the optimum poling conditions were at 4.0 kV/mm of the electric field (Fig. 2.21) for 45 min (Fig. 2.22) with the poling temperature of 120°C (Fig. 2.23). With the increase of the PZT content, the d_{33} and g_{33} increased nonlinearly (Fig.

2.24). For the particle sizes under 130 μm , the d_{33} increased at a faster rate with increasing particle size of PZT, whereas the d_{33} value was nearly size independent when the size was larger than 130 μm . Moreover, the electromechanical coupling coefficient of the composites (k_p and k_t) increased rapidly with increasing PZT contents (Table 2.8).

Furthermore, in 2006 Shifeng *et al.* [84] investigated suitable conditions for optimum value of the composite properties. They used ten kinds of lead lithium niobate-lead zirconate-lead titanate (PLN) particles with different average particle size to form cement-based piezoelectric composites and the PLN mass fraction was 80% in all piezoelectric composites. From their results, it was shown that piezoelectric strain factor (d_{33}) and piezoelectric voltage factor (g_{33}) both increased with increasing the PLN particle size.

Moreover, it was seen that when the PLN particle size was larger than 100 μm , d_{33} and g_{33} were hardly influenced by the PLN particle size. It was believed that, because of decreasing the PLN particle size, the surface area and volume ratio of the PLN particle increased, which resulted in the low piezoelectric properties or non-piezoelectric properties of the surface layer. Furthermore, since the chances for the larger ceramic particles to contact each other increased, the connectivity patterns of composite also changed (the result are showed in Fig. 2.25). Moreover, in the same year (2006) Shifeng *et al.* [15] studied the 0–3 sulphoaluminate cement based piezoelectric composites prepared by compressing technique. A further goal was to establish the optimum poling conditions and to analyze the reasons that affect the degree of the poling. The poling was carried out under different poling conditions in a stirred silicone oil bath. In each kind of piezoelectric composite, the contents of PZT

were 60, 70, 80 and 85 wt%. The result exhibited that, in the course of the poling, the leakage current was chiefly caused by the interface pore, the cement matrix pore and their inner water which has a significant influence on the degree of the poling. The interfacial bonding between PZT and cement are showed in Fig. 2.26.

From the previous works, it is seen that the important PZT ceramic was paid attention from many researchers to mix with Portland cement. However, some researchers work on complex perovskite piezoelectrics. In 2005, Xin *et al.* [85] studied 0–3 piezoelectric using a sulphoaluminate cement and PMN ceramic particles. Piezoelectric and dielectric properties of the composites with different PMN contents were investigated. The specimens were put in a curing room with a temperature of 20°C and relative humidity of 100% for 3 days before measurements.

Then, the poling was carried out at 130°C in a stirred silicone oil bath. The result showed that the optimum poling field was 4kV/mm for all samples. The d_{33} values of the 0–3 cement-based piezoelectric composites showed a roughly nonlinear increase as a function of the PMN content. Moreover, the addition of PMN particles changed the electromechanical coupling behavior to the composites. The K_p and K_t values of the composites increased with increasing the PMN content and the Q_m value was in the range from 19.84 to 40.41. Additionally, the piezoelectric properties of the composites were improved with increasing the hydration age and d_{33} tended to be constant when the cement hydration age exceeded 8 days as shown as in Fig 2.27.

Furthermore, Xin *et al.* [86] investigated 0–3 piezoelectric ceramic/sulphoaluminate cement composites with 50–75% P(LN)ZT volume fractions. The piezoelectric, dielectric, and ferroelectric properties of the composites were especially studied. The results showed that the piezoelectric strain factor (d_{33}), the dielectric constant (ϵ_r) and

dielectric loss increased as the P(LN)ZT volume fraction increased, which followed the cube model well.

In addition, in 2009, Shifeng *et al.* [87] studied effect of carbon black on properties of 0–3 piezoelectric ceramic/cement composites. The composites were fabricated using sulphoaluminate cement and piezoelectric ceramic [P(LN)ZT] as raw materials and were investigated the influences of carbon black content on the piezoelectric, dielectric properties and electric conductivity, respectively. The result indicated that the carbon black addition brings improvement in piezoelectric strain constant d_{33} and piezoelectric voltage constant g_{33} of the composites as shown in Fig. 2.28 and they explained that when adding a small amount of conductivity phase such as carbon to the composites, the impedance of the composites is decreased and the electric conductivity is increased. Accordingly, the electric conductivity of the cement matrix is raised. This in turn increases the electric field on the ceramic particles making poling more easily. Therefore, the piezoelectric strain constant d_{33} increases gradually with a suitable carbon black addition.

Moreover, the dielectric constant, ϵ_r and dielectric loss, $\tan \delta$ of the composites increase as the carbon black content increases (Fig. 2.29). From these results, they can be illustrated that carbon black exists in the composites as tiny grains, just as introduces a lot of tiny capacitors. The more carbon black content, the more tiny capacitors introduced. Therefore, the higher dielectric constant appears in the composites with higher content of the carbon black while with the increase of carbon black content, the dielectric loss $\tan \delta$ of the composites also increases. It can be due to the fact that the electric conductivity of the composites increases sharply with

increasing the carbon black content, which results in the increases of the dielectric loss.

At the same year (2009), Gong *et al.* [88] also studied piezoelectric and dielectric behavior of 0-3 cement-based composites mixed with carbon black. However, they fabricated the composites system using carbon black/PZT/cement which consists of white cement as a matrix, homogeneously distributed PZT particles as a ferroelectric phase, and carbon black added as a conductive phase. The aging and poling conditions of the composites were investigated and the influences of carbon addition on the dielectric and piezoelectric properties of the composites are also examined.

The results were shown that (Fig. 2.30) the use of a conductive carbon black phase can facilitate the poling process at room temperature. The d_{33} values of the composites fluctuated at the initial stage of the aging process (Fig.2.31), possibly due to the temporarily aligned dipoles in the cement matrix whose conductivity was enhanced by the introduced carbon black. For enhancing the dielectric and piezoelectric properties of the composites, they found that a limited amount of carbon black additive optimum of about 1.0 vol% and the results were shown in Fig 2.32. However, the piezoelectric activities of the composites reduced due to its excess electric conductivity as carbon black.

From these previous literatures, there are a lot of works on composites between PZT or PMN and Portland cement, especially on the piezoelectric properties of the composites. However, the 0–3 connectivity cement-based piezoelectric composites is still difficult to obtain good piezoelectric properties due to the difficulty in poling ceramic particles in such composites because of the presence of some pores in a

composite. Moreover, in the course of the poling, the leakage current is still chiefly caused by the interface pore, the cement matrix pores and their inner water, which has a significant influence on the degree of the poling. The effective way to improve poling degree is to eliminate these pores which can be implemented by enhancing compact press or adding admixture such as water reduction and antifoaming to the cement matrix and drying the samples in a vacuum box. And another way to improve effectively poling of piezoelectric ceramic is to add insulator phase between piezoelectric particles by an introduction of a small volume fraction of a third phase.

Table 2.6 Properties of composites [7]

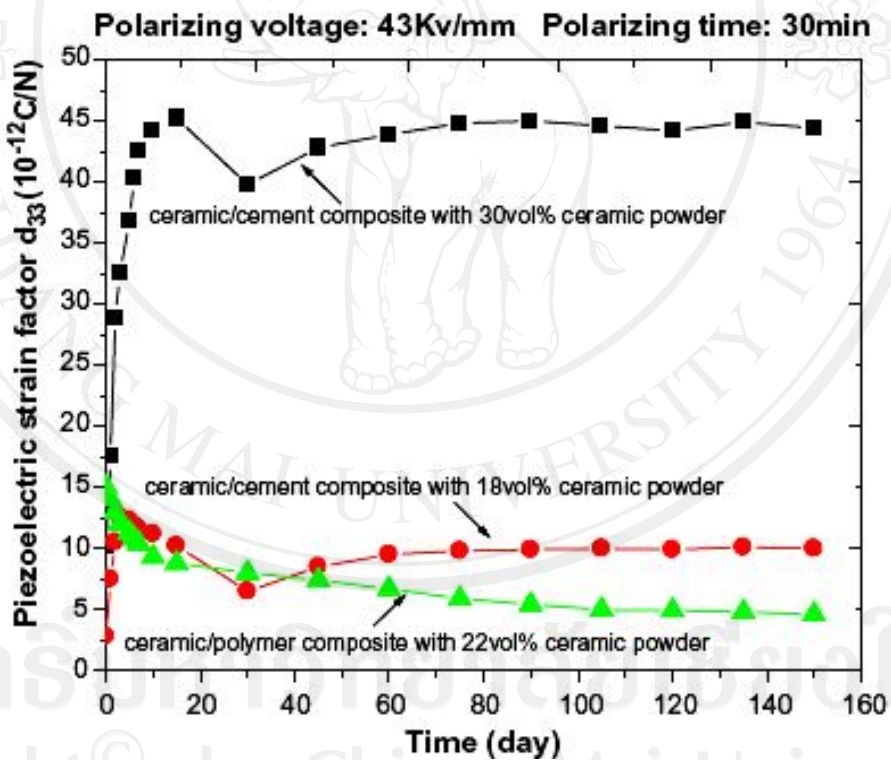
Specimen code	PZT particle type	PZT particle content (vol%)	d_{33} (10^{-12} C/N)	g_{33} (10^{-3} Vm/N)	k_t	ϵ_r
a	PZT I	35	7.2	18.6	11.6	43.5
b	PZT I	50	9.5	16.8	12.9	63.9
c	PZT I	65	18.0	22.1	18.6	92.1
d	PZT II	35	8.1	15.1	12.9	60.7
e	PZT II	50	12.5	15.0	13.2	94.2
f	PZT II	70	33.4	20.7	20.7	182.2
Matrix		0				26.2

Note: PZT I, Mean dia. =6.45 μ m, Median dia. = 4.92 μ m

PZT I, Mean dia. =153.6 μ m, Median dia. = 83.52 μ m

Table 2.7 Piezoelectric parameter of the 0-3 nano-PZT/cement composites [83]

PZT particle content (vol%)	Piezoelectric strain factor, d_{33} (pC/N)	Electromechanical coupling coefficient, k_t	Relative dielectric constant, ϵ_r
35	7.3	10.1	21.2
50	18.5	10.5	83.4
65	29.7	12.6	112.8
80	53.7	18.1	130.5

**Fig 2.20** Aging influence on piezoelectric factor (d_{33}) for cement-based piezoelectric composites and ceramic/polymer composites [78]

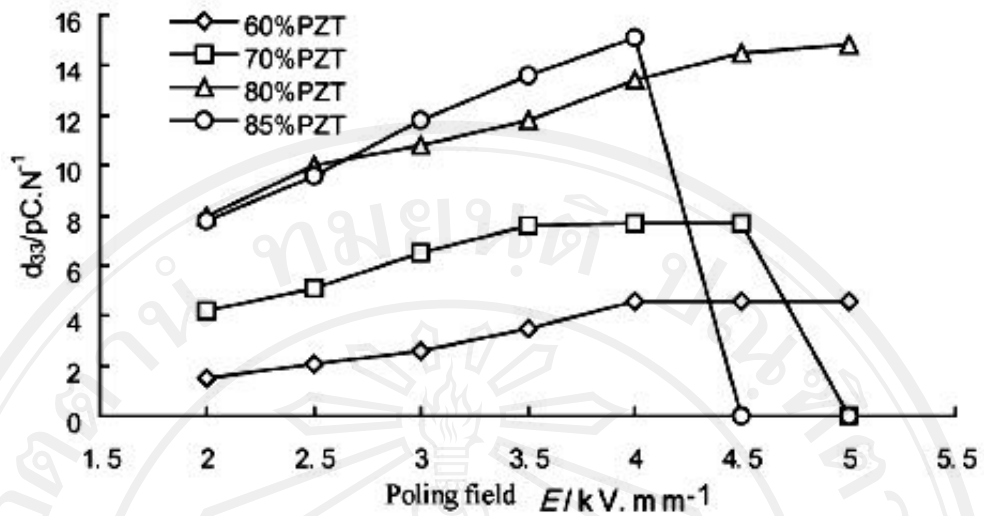


Fig 2.21 The piezoelectric strain factor (d_{33}) of the composites as a function of the poling field E [80]

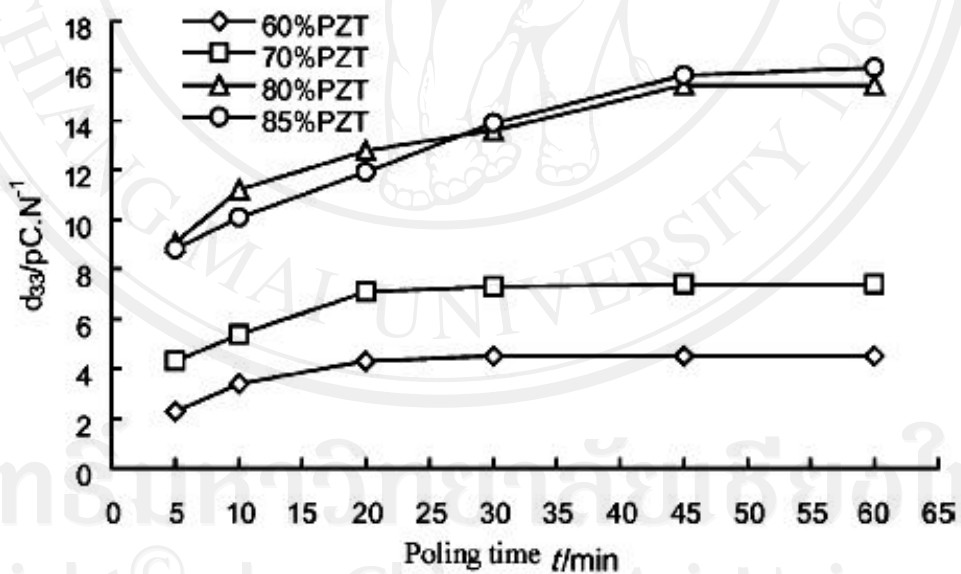


Fig 2.22 The piezoelectric strain factor (d_{33}) of the composites as a function of the poling time t [80]

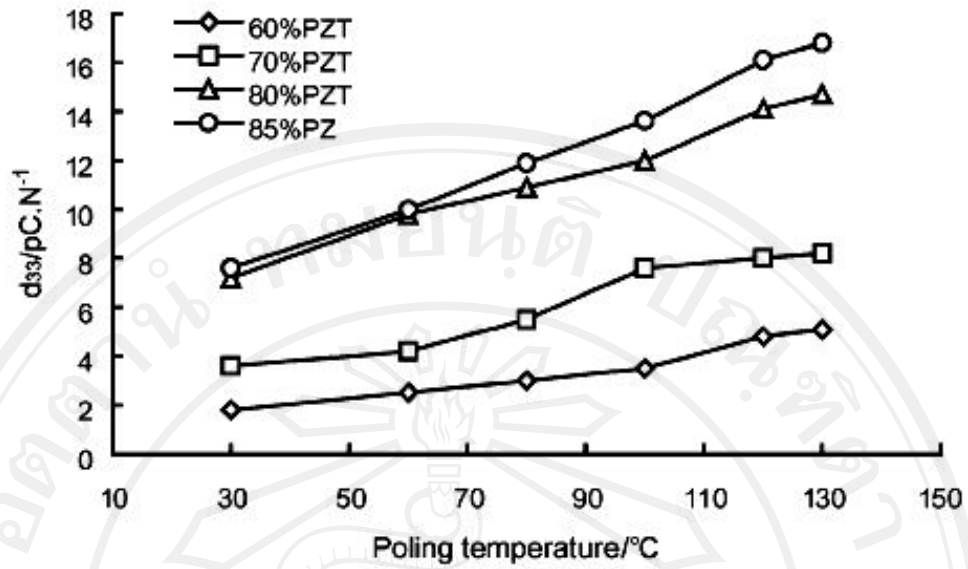


Fig 2.23 The piezoelectric strain factor (d_{33}) of the composites as a function of the poling temperature T [80]

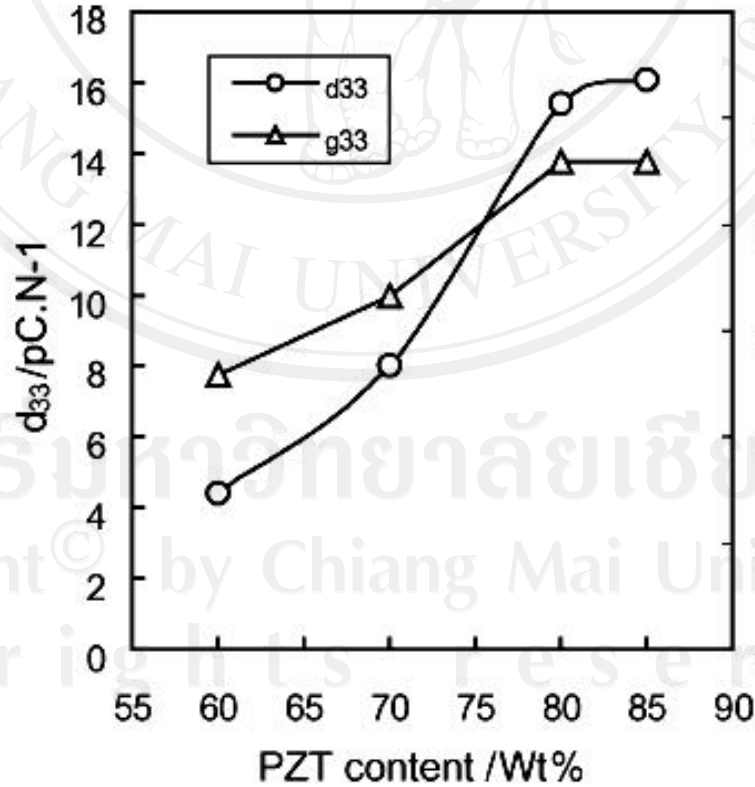


Fig 2.24 Dependence of the piezoelectric constants on the content of PZT [80]

Table 2.8 The electromechanical coupling properties of the composites [80]

PZT content wt (%)	f_m (kHz)	f_n (kHz)	Δf (Hz)	k_p (%)	k_t (%)
60	227.53	228.78	1250	11.79	11.57
70	230.03	232.53	2500	15.76	16.19
80	208.78	211.28	2500	17.20	16.97
85	145.03	150.03	5000	28.54	28.19

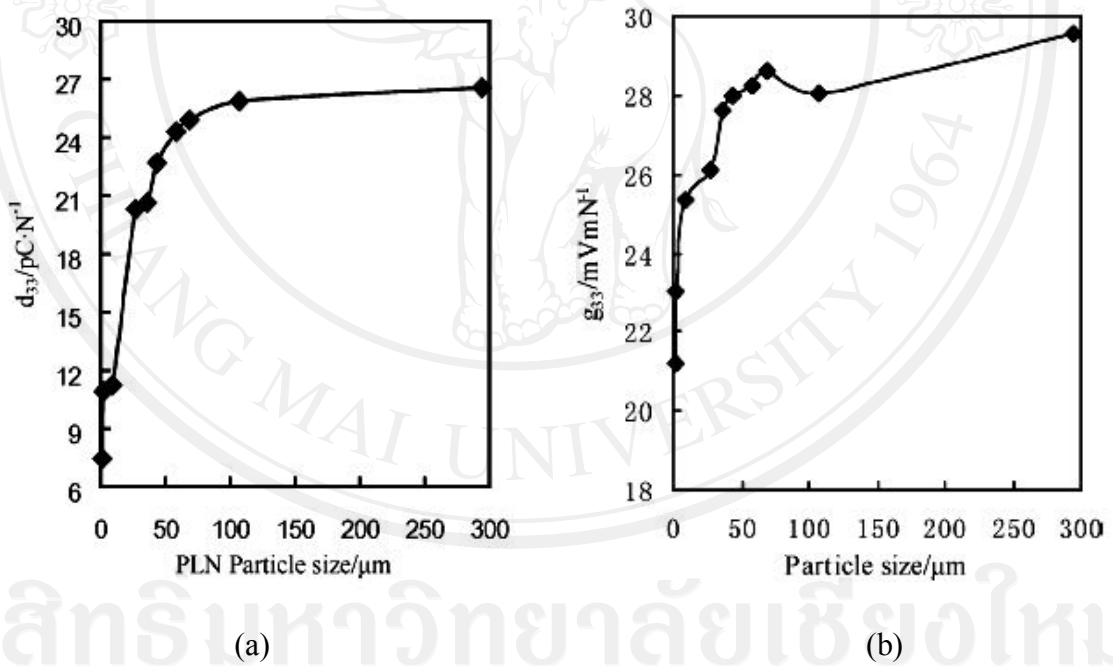


Fig 2.25 Effect of PLN particle size on piezoelectric properties of the composites; (a) Piezoelectric strain factor (d_{33}), and (b) Piezoelectric voltage factor (g_{33}). [84]

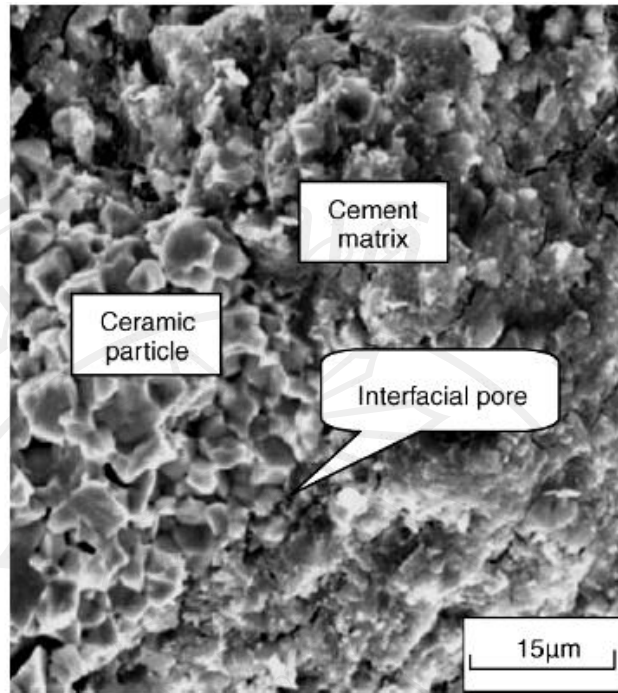


Fig 2.26 The interfacial bonding of the PZT ceramic particle and the cement matrix

[15]

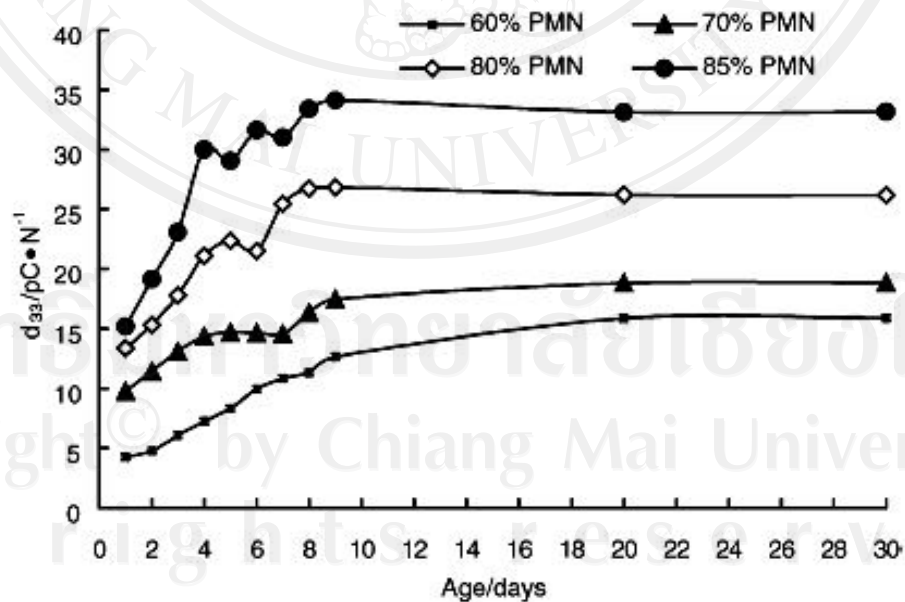
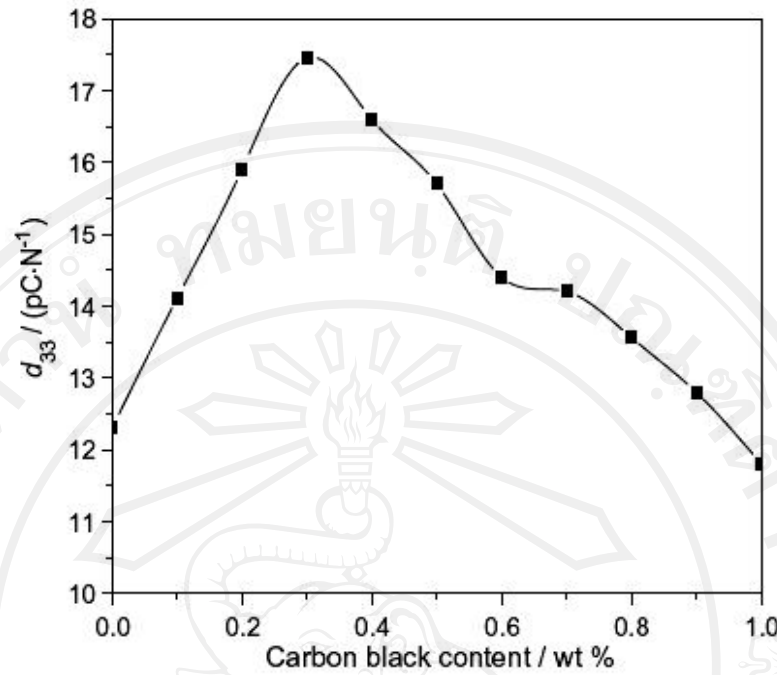
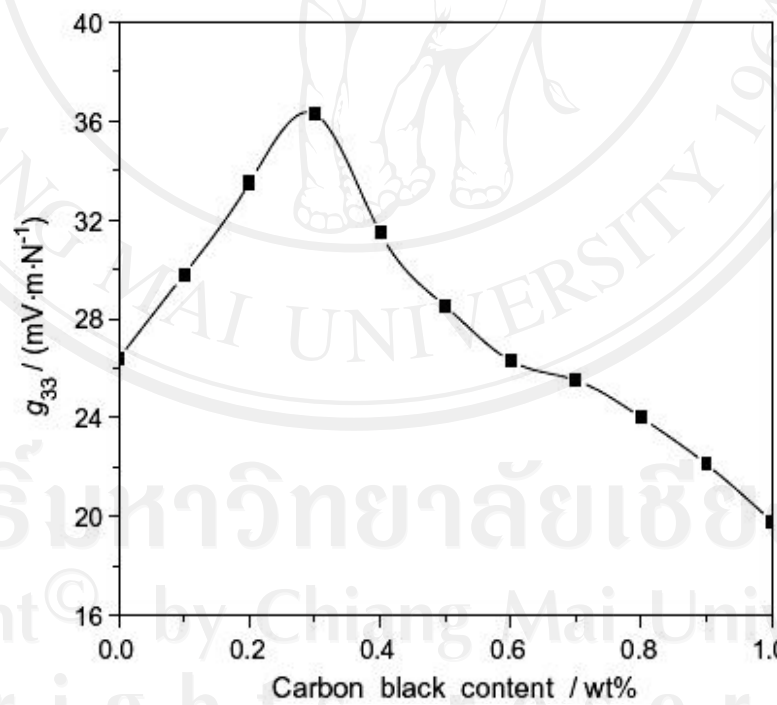


Fig 2.27 The influence of ages on the piezoelectric strain factor (d_{33}) constant of the composites [85]

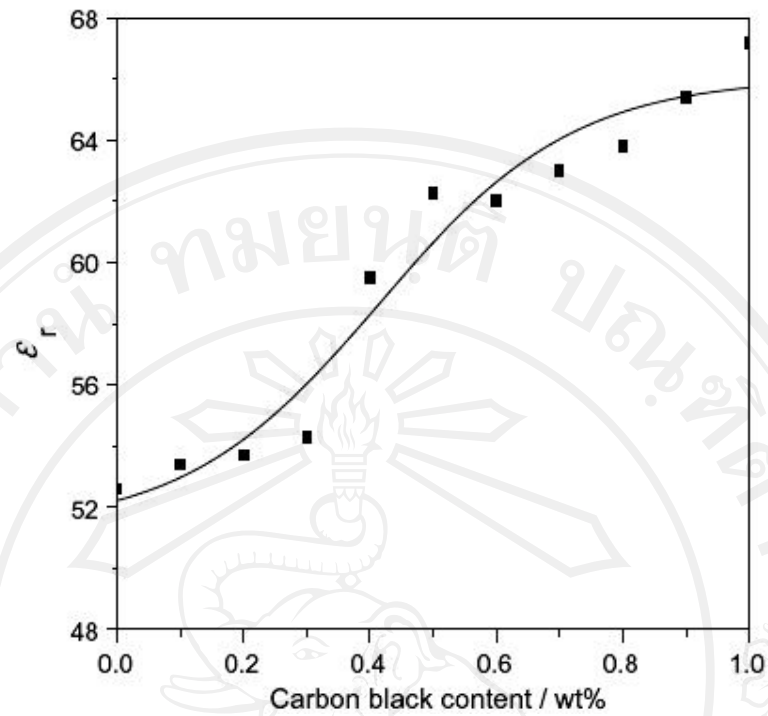


(a)

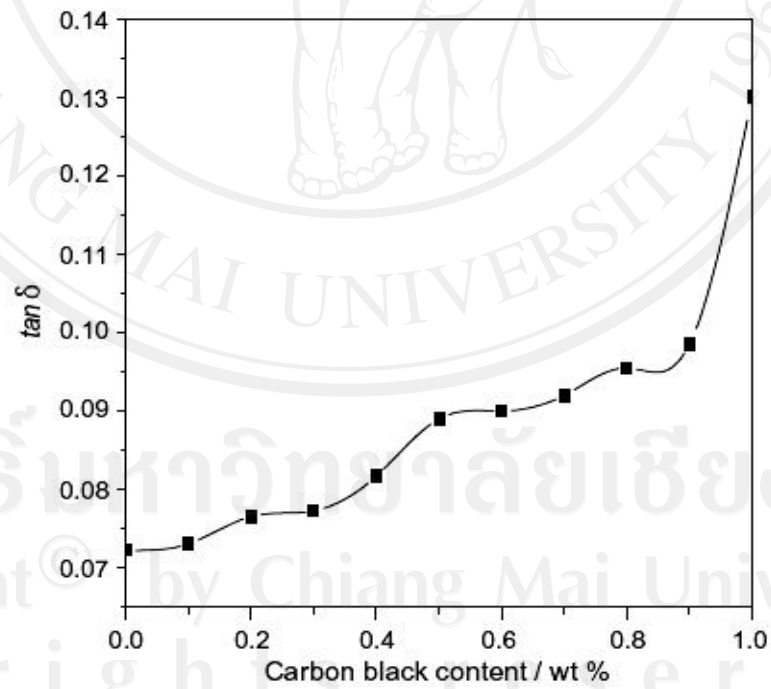


(b)

Fig 2.28 Variation of piezoelectric strain constant (d_{33}) (a), and piezoelectric voltage constant (g_{33}) (b), of the composites with carbon black content [87]

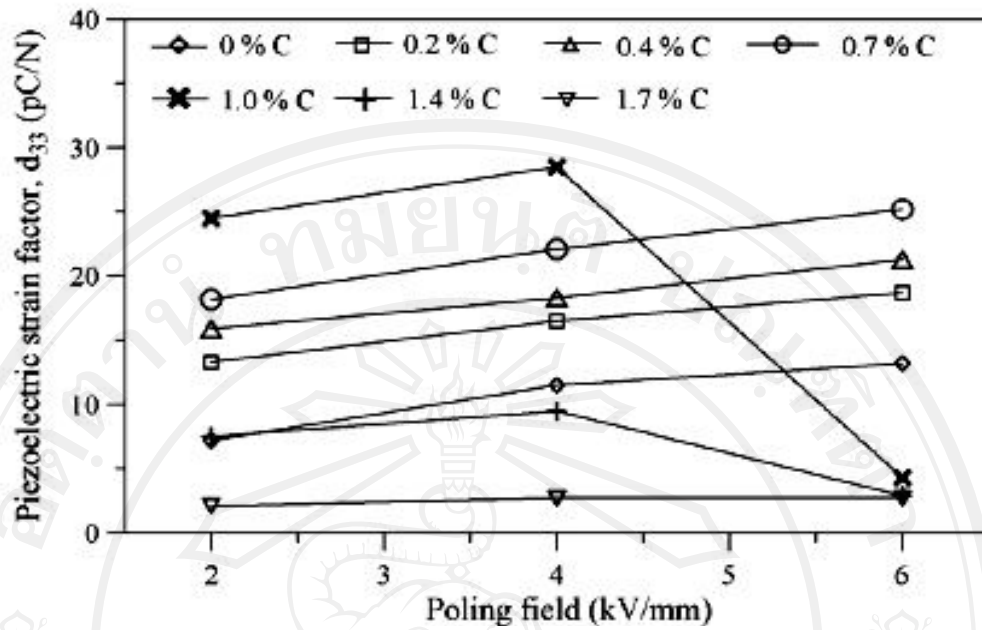


(a)

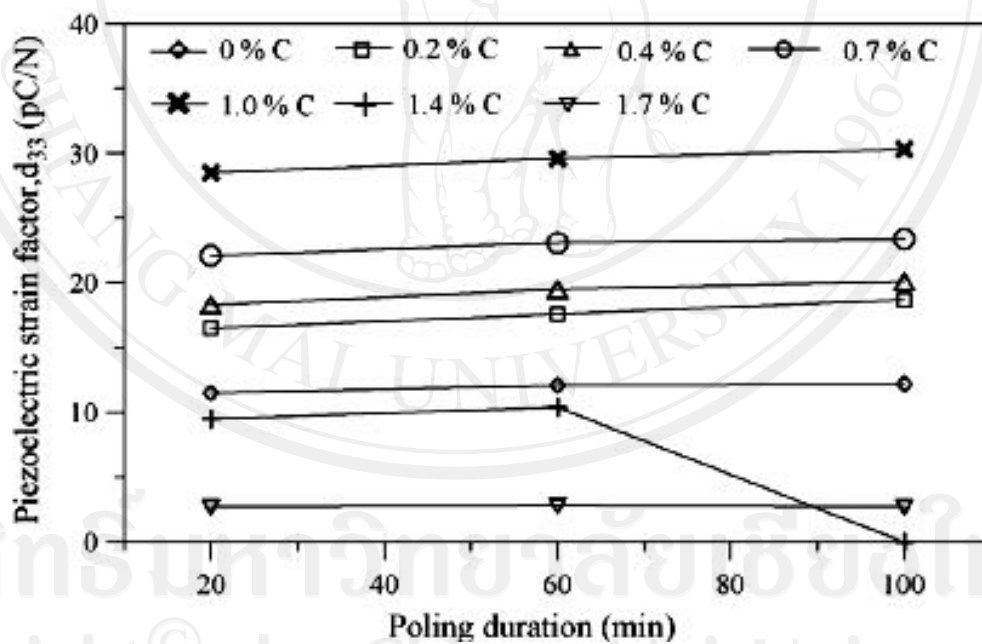


(b)

Fig 2.29 Variation of dielectric constant (a), and dielectric loss (b), of the composites with carbon black content [87]



(a)



(b)

Fig 2.30 Dependence of the piezoelectric strain factor (d_{33}) of the carbon black /PZT/cement composites on the poling field (a), and on the poling duration (b) [88]

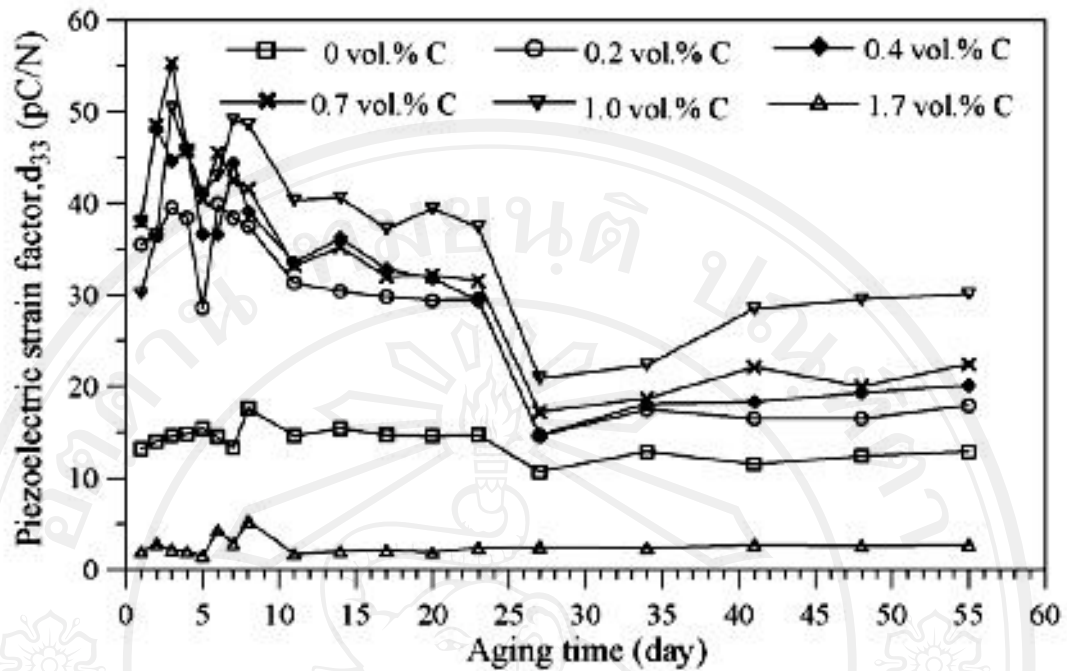
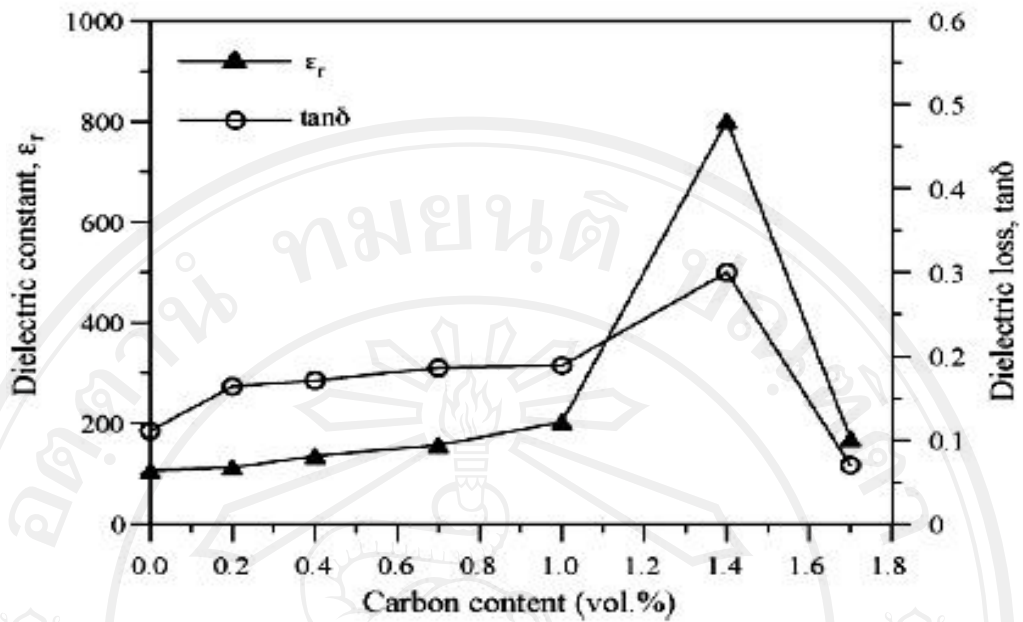
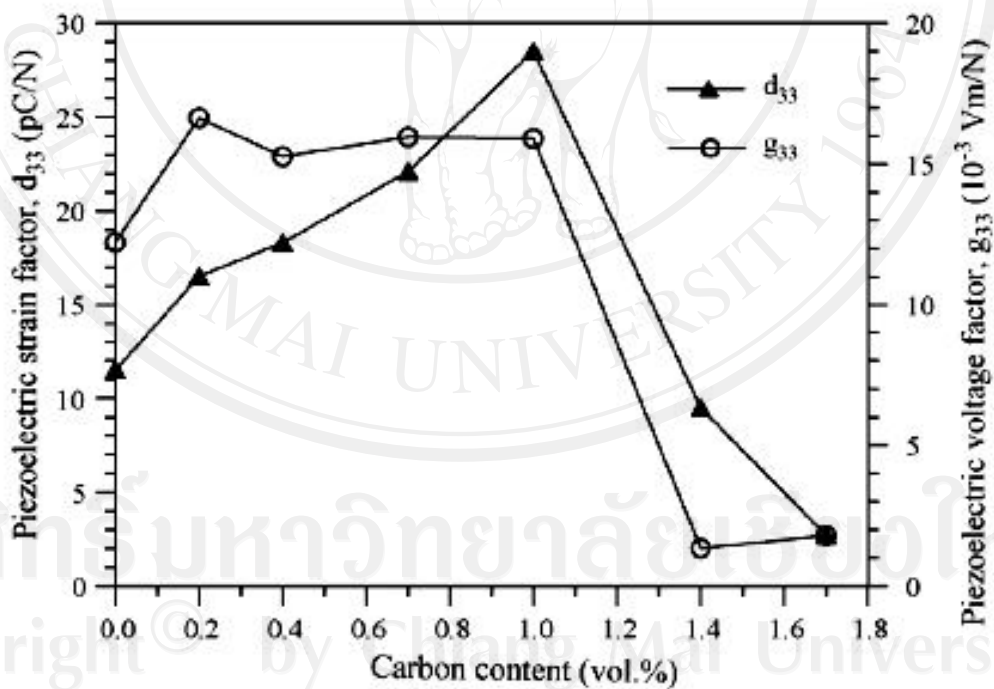


Fig 2.31 Variations of piezoelectric strain factor (d_{33}) of the composites with the aging time [88]



(a)



(b)

Fig 2.32 Dependence of (a); the dielectric constant (ϵ_r) and dielectric loss ($\tan \delta$) and (b); the piezoelectric strain factor (d_{33}) and piezoelectric voltage factor (g_{33}) of the carbon black/PZT/cement composites on the carbon content [88]